Channel Estimation and Soft OSIC Detection in Coherent MIMO-OFDM Systems Using QRD Techniques(802.16m)

by

Divyang Rawal

A THESIS SUBMITTED IN PARTIAL FULFILMENT OF THE REQUIREMENTS FOR THE DEGREE OF

Doctor of Philosophy

IN

INFORMATION AND COMMUNICATION TECHNOLOGY

TO

DHIRUBHAI AMBANI INSTITUTE OF INFORMATION AND COMMUNICATION TECHNOLOGY

JANUARY 2013

Declaration

This is to certify that

1. the thesis comprises my original work towards the degree of Doctor of Philosophy in Information and Communication Technology at DA-IICT and has not been submitted elsewhere for a degree,

2. due acknowledgment has been made in the text to all other material used.

Signature of Student

Certificate

This is to certify that the thesis work entitled "Channel Estimation and Soft OSIC Detection in Coherent MIMO-OFDM Systems Using QRD Techniques (802.16m)" has been carried out by Divyang Rawal (200521001) for the degree of Doctor of Philosophy in Information and Communication Technology at this Institute under my supervision.

Thesis Supervisor Prof. Vijaykumar Chakka

Abstract

Next generation mobile systems will use multiple antennas at the transmitter and receiver to achieve higher capacity and diversity gain at high speeds. By transmitting through multiple transmitting and receiving antennas, multiple wireless data pipes are created. A transmitted signal while propagating through the wireless channel, undergoes multipath fading effect accompanied by noise and interference. Mitigation of these effects and increase in throughput is only possible if the channel is accurately estimated at the receiver in order to perform coherent detection. Existing literature mentions both coherent and noncoherent detection. However, here the work focus on coherent detection due to its advantages of low power transmission and less complex transmitting and receiving methods compared to noncoherent detection. Coherent detection consists of two steps; the first one being channel estimation and the second is data detection.

As a first step of Coherent Detection in MIMO systems, different channel estimation methods are investigated. Literature describes pilot assisted as well as blind methods in terms of performance, spectral efficiency, convergence speed and complexity. Depending on slow/fast channel fading conditions, several authors suggested adaptive MMSE, LS, LMMSE, RLS based pilot channel estimators, which either require statistical information of the channel or are not efficient enough in terms of performance or computations.

In order to overcome the above effects, the work focuses on the QR-RLS based channel estimation method for MIMO-OFDM systems. The proposed estimator uses preamble for time domain channel tracking, thus avoiding error spreading over the whole band as in its frequency domain conterpart. Use of RLS avoids the need for channel statistical information like MMSE, LMMSE estimators while the use of QR decomposition also avoids matrix inversion as in RLS estimators. For low and moderate channel fading condition, the proposed estimator is used in DDCE(Decision Directed Channel Estimator) mode. In this, the first order markov model is used in conjucion with the proposed estimator to estimate channel variations, symbol by symbol. For improving performance in a fast fading environment, the work is advanced for QR-LS based joint coarse-fine channel estimation. In the proposed work, QR-RLS estimated coarse channel component is used jointly with scattered frequncy domain pilots for fine symbol by symbol channel estimation. The proposed method gives better performance compared to pilot interpolation based estimators.

Moving to the second step of Coherent Detection, spatial multiplexing (SM) is a technique to increase throughput by allowing multiple spatial streams in MIMO systems. At the receiver, MIMO streams are separated using linear or VBLAST/OSIC detectors. Literature compares linear as well as OSIC detectors in terms of performance and complexity. Many authors have suggested optimal QR based OSIC detectors which achieve hard ML(Maximum Likelihood) performance but

suffer from Empty Vector Set(EVS) problem while achieving soft ML performance. EVS problem is more severe in terms of performance when the modulation order is low. Several remedies have been described by many authors to mitigate EVS. However, they fall short in terms of performance or complexity while achieving Soft ML performance.

To mitigate Empty Vector Set(EVS) problem effectively, two solutions are proposed here. In the first one, an enlargement of candidate vector set of QRLRL(QR - Least Reliable Layer) based MIMO detector for efficient soft output generation is proposed. The overall enlarged candidate vector set consists of vectors with every constellation point tried at each layer. The proposed detector thus effectively removes EVS problem and achieves soft ML performance while keeping the computation complexity low at low modulation order. QR-LRL based IDD(Iterative Detection and Decoding) is another solution, which exchanges the extrinsic information between detector and decoder. Based on feedback knowledge from the decoder, a decision is made to update candidate vector set for soft output generation. Simulation results show that significant performance improvement is achieved while keeping the receiver design simple.

Thesis contribution:

1. A novel method for OFDM-MIMO channel estimation using QR-RLS(Square Root-Recursive Least Square) estimator is presented.

2. QR-RLS based MIMO(Multiple input Multiple output) channel estimation is combined with scattered pilots for coarse-fine channel estimation in Mobile Wimax 802.16m system.

3. MIMO OSIC detectors suffer from EVS(Empty Vector Set) problem while generating soft output. Two solutions are proposed to mitigate EVS.

   (a) Candidate Vector set of QR-LRL MIMO detector is effectively enlarged to mitigate empty vector set problem and achieve soft ML performance.

   (b) QR-LRL based SM-MIMO detector is iteratively used with TURBO decoder to achieve soft ML performance without adding any extra computational complexity to the receiver.

Acknowledgments

It gives me great pleasure to acknowledge several of the many people who have supported me on my journey through the Ph.D. program. They provided me with some insightful suggestions, witty criticism, professional-academic advice and support in each and every way. The rewards in waiting to see this day are undoubtedly sweet. I owe this to my family, friends, professors and DA-IICT. It is an honor to express my sincere, deepest, heartfelt gratitude to the people mentioned here and to many others.

First and foremost, I would like to thank my thesis advisor, Prof. C. Vijaykumar for many insightful conversations and helpful comments during the development of the ideas in this thesis. With his inspiration, desire to share knowledge, expression of excitement in gaining new scientific insights and great efforts to explain things simply and clearly, he helped me enjoy doing the thesis work. It was a great learning experience being his student as well as teaching assistant.

I was delighted to interact with Prof. Manjunath Joshi by attending his classes and having him as my thesis committee member. I developed insightful ideas about signal processing "How Things Work/Make them work" during his classes on Image processing. I would like to thank Prof V.P. Sinha and Prof. Samaresh Chatterji for making the complex math-world simple for me, especially linear algebra. I would like to thank Prof. Suman Mitra for improving my understanding of signal statistics.

I would like to specially thank Sunil and Nitin who inspired me at my Ph.D. commencement and then supported me throughout. I also would like to thank Nilesh and Purushothaman for the nice talks and subjective/objective knowledge support. I also thank my fellow labmates : Ratnik, Pratik, Jignesh, Gunesh, Bhavesh, Shubham and Gannu for the stimulating discussions and for sleepless nights while working together to meet deadlines and for all the fun we had in the last several years.

I would like to thank my Team Leader, Park Youn Ok for giving me a chance to become a part of a real time project on development of WiBro systems, as a part of my Industrial exposure. He let me gain, develop and stimulate my research on novel platforms. I am very thankful to my teamebers Changwahn Yu and David Junghyun Kim for their support in the overall Wimax system development. I would also like to thank my team members, Hoon Lee, Hyeong Sook Park and Seungjae Bahng for their inspirational ideas, discussions of novel techniques and knowledge sharing attitude.

Last, but not the least, I would like to dedicate this thesis to my whole family especially my grandmother, Indumati, my wife, Foru and daughter, Naavya, for their love, patience and understanding.

Contents

List of Figures

List of Tables

List of Abbreviations

CIR	**C**hannel **I**mpulse **R**esponse
CP	**C**yclic **P**refix
CRU	**C**ontinuous **R**esource **U**nit
DDCE	**D**ecision **D**irected **C**hannel **E**stimator
DFE	**D**ecision **F**eedback **E**qualizer
DLRU	**D**istributed **L**ogical **R**esource **U**nit
EVS	**E**mpty **V**ector **S**et
FEQ	**F**req-Domain **E**qualizer
ISI	**I**nter **S**ymbol **I**nterference
ICI	**I**nter **C**arrier **I**nterference
IDD	**I**terative **D**etection and **D**ecoding
LSE	**L**east **S**quare **E**stimator
LMS	**L**east textbfMean **S**quare
LLR	**L**og-**L**ikelihood **R**atio
LMMSE	**L**inear **M**inimum **M**ean **S**quare **E**stimator
LRL	**L**east **R**eliable **L**ayer
MIMO	**M**ultiple **I**nput **M**ultiple **O**utput
ML	**M**aximum **L**ikelihood
MMSE	**M**inimum **M**ean **S**quare **E**stimator
MRL	**M**aximum **R**elaiable **L**ayer
OFDM	**O**rthogonal **F**requency **D**ivision **M**ultiplexing
OSIC	**O**rdered **S**uccessive **I**nterference **C**ancellation
PHY	**PHY**sical layer
PSAM	**P**ilot **S**ymbol **A**ssited **M**odulation
RLS	**R**ecursive **L**east **S**quare
PRU	**P**hysical **R**esource **U**nit
SA/PA	**S**econdary **A**dvanced/ **P**rimary **A**dvanced
SM	**S**patial **M**ultiplexing
STBC	**S**pace **T**ime **B**lock **C**ode
TEQ	**T**ime-Domain **E**qualizer
VBLAST	**V**ertical **B**ell labs **L**ayerd **S**pace **T**ime
WLAN	**W**ireless LAN
WiMax	**W**orldwide **I**nteroperability for **M**icrowave **A**ccess
ZF	**Z**ero **F**orcing

Chapter 1

Introduction

1.1 MIMO OFDM Systems

In recent years, Internet usage has increased in leaps and bounds and has billions of users. Internet usages like VOD-Video On Demand, E-Mail, Browsing, Contacts etc...demand high speed Internet that leads to a need for broadband adoption. At the same time, cellular systems have made it possible for people to stay connected with the world from almost anywhere, resulting in a concept while $OnTheMove$. With the increase in users and their demands, the broadband market continues to grow, which in turn leads to development of new technologies like Wimax [1], LTE, LTE-advanced for broadband wireless. These technologies provide usage flexibility, high throughput and more coverage.

Wireless channel[42] is the main barrier for these new technologies. It causes impairments like noise addition, interference, multipath fading effects etc. in the transmitted signal. This demands very complex algorithms in the wireless receiver to overcome these impairments. Previous technologies like GSM[45] use FDM(Frequency Division Multiplexing), while CDMA uses orthogonal codes and spread spectrum to overcome channel impairments. These systems have their own limitations. For example, FDM requires guard band for separation to overcome interference between two consecutive users. Similarly, CDMA[45] needs to generate orthogonal sequences with zero correlation which is difficult to achieve if the number of users increases indefinitely. This leads to OFDM[31][66] (Orthogonal Frequency Division Multiplexing). The concept is equivalent to dividing the channel frequency response into smaller orthogonal subbands. Since each adjacent frequency is orthogonal to each other, it eliminates the need of guard band for separation. Simultaneously, OFDM divides high data rate signal into multiple small data rate signals. Moreover, it can be implemented by simple FFT/IFFT techniques, leading to ease in implementation.

OFDM systems generally use CP(cyclic prefix) between two consecutive OFDM symbols to prevent ISI(Inter Symbol Interference). However, use of CP reduces spectrum efficiency. In existing literature, various methods like front end TEQ (Time domain Equalization) and channel shortening methods are proposed to reduce CP size. However, such TEQ suffers from noise amplification problem and gives poor performance in highly correlated channel environments. An alternative method to mitigate channel effects is providing sufficient CP and 1 tap FEQ(Frequency domain Equalization). In this method, the channel is estimated using preamble/pilot symbols. The estimated channel is then used in FEQ to eliminate or partially mitigate channel effects.

Fading can also be overcome by using diversity techniques like space, time, frequency and transmit diversity. Multiple versions of data are transmitted by using any of these parameters. The receiver receives multiple versions of the same data under different fading conditions. At the receiver, different combining methods like MRC(Maximal Ratio Combining), SC(Selection Combining) etc. are used to overcome narrowband fading with the help of array and/or diversity gain. Especially space diversity can be used to achieve high throughput/diversity gain by using a multiple transceiver antenna system, which creates multiple data pipes in the wireless channel. This results in multiple of Shannon capacity under favorable conditions. Such systems are called MIMO systems.

The two systems mentioned above, merged to a single system and gave robust performance and high throughput under wireless fading environment resulting in MIMO-OFDM systems[4]. Generally, MIMO-OFDM systems use CP of sufficient length to avoid ISI. For reliable demodulation of the transmitted data, a receiver mitigates channel impairments like signal attenuation and phase distortion. Such a reception strategy encourages reception methods called coherent demodulation [41]. There are some other methods also available for data demodulation even without compensating the channel distortions by suitably adapting the transmission modulation. Such a reception scheme called non-coherent demodulation[41][56], is inferior compared to coherent demodulation in terms of the bit error rate (BER) achieved for a given amount of transmit power [57]. For this reason, coherent reception is preferred in mostvof the modern communication systems.

1.2 Coherent Detection Requirement 1: Channel Estimation

Coherent demodulation acquires channel knowledge at the receiver to compensate for the channel induced distortions. The process of acquiring the channel knowledge is called channel estimation which is an integral part of most of the communication receivers nowadays. Apart from the knowledge of channel statistics, the channel estimator also requires knowledge of the instanta-

neous channel values to track the channel fading and compensate it. Available literature generally describes two types of channel estimation methods. One is based on pilot based estimation and the other is blind estimation[58][68]. Blind channel estimation methods avoid the use of pilots and have higher spectral efficiency. However they suffer from high computational complexity and low convergence speed required to derive statistical information from received data. On the other hand, pilot based estimation uses pilots in block/distributed manner, depending on channel slow/fast fading conditions. The transmitter transmits multiplexed $pilot$ symbols along with data symbols to acquire channel knowledge at the receiver. Such a channel estimation scheme is called Pilot Symbol Aided Modulation (PSAM). The estimator then uses sophisticated signal processing algorithms like LSE and MMSE to acquire the channel knowledge using pilot symbols.

Several authors have proposed channel estimation in frequency domain[63][35][8] for OFDM systems using MMSE and LSE methods. However MMSE methods require prior knowledge of channel statistics. Such information is not generally known which leads to modified LMMSE based method. Still this method requires higher computations.On the other hand, LSE based method requires just a scalar division to estimate the channel in frequency domain, but it leads to high channel estimation MSE error since the estimation error gets spread over the whole frequency band. This leads to time domain channel estimation which is more robust as it tracks down the inherent frequency correlation among the taps.

Literature also addresses[51][20][13][55][27] time domain channel tracking methods like MMSE, LMS, RLS adaptive estimators for OFDM systems. These methods use training symbols for estimator coefficient updating. The author[14] suggested different methods according to their convergence time and estimation error. As mentioned earlier, MMSE requires prior knowledge, while LMS method only use currently received value for filter coefficient updating, resulting in slow convergence. Filter updating based on a block of received data is more accurate, fast converging and also averages out the noise effect. Such methods are called RLS based channel tracking. Still RLS based updating suffers from high computation due to matrix inversion and singularity under highly correlated channel conditions. This leads to proposed QR-RLS based channel estimation for MIMO OFDM systems, which use preamble symbols for initial channel estimation. Literature[27] shows use of DDCE method where first order Markov model is used for symbol by symbol channel tracking after initial estimate. The above method produces better results in low and moderate channel fading environments.

Under fast fading channel conditions, performance improvement is achieved by using time domain QR-RLS channel estimator in-conjunction with scattered pilots in frequency domain. Literature [21] shows cases of only pilot based estimation where either Block, COMB, scattered pilots are transmitted. Generally under fast fading conditions for doubly selective channels, pi-

lots are scattered with period of coherence bandwidth and coherence time. Various interpolation techniques[7] like linear, spline, 2D wiener based methods are then used for channel estimation using scattered pilots. Since pilot based estimation is merely a frequency domain estimation, performance is improved by combining QR-RLS based coarse channel estimation with pilot based fine estimation.

1.3 Coherent Detection Requirement 2 : MIMO Data Detection

Once the channel is estimated, the next step in coherent MIMO system is to detect the correct symbols. Use of multiple antennas for transmission leads to various gains like array gain, diversity gain,etc.[40]. While array gain and diversity gain provide system reliability and increase the coverage area or decrease the required transmit power, SM (Spatial Multiplexing) increases the achievable data rate and hence the system capacity. Unfortunately, the Spatial De-multiplexing at the receiver is a challenging task.

Maximum Likelihood (ML) decoding achieves good error performance. However, its computational complexity increases exponentially with regard to the number of transmit antennas or spatial streams. On the other hand, linear filtering approaches such as Zero Forcing (ZF) or Minimum Mean Squared Error (MMSE) detection require low complexities. But their error performance is poor due to noise enhancement in the filtering process. VBLAST(Vertical Bell labs), an OSIC(Ordered Successive Interference Cancellation) method is an optimal solution in terms of complexity and performance. A lot of research has been done in OSIC based detection method. Since the conventional OSIC detectors detect symbols successively, it suffers from error propagation if the correct symbol is not found at the first layer. However, QR-LRL based OSIC guarantees minimum error propagation among all the OSIC detectors and achieves hard ML performance. But it suffers from Empty Vector Set problem while achieving soft ML performance.

Several remedies are addressed in the literature [54][26][16]. These include (i) deriving threshold value from non-suffering EVS layer, (ii)deriving log likelihood function from the remaining candidate vectors for non-existing bits and (iii) use of multiple QR decomposition structure for trying every constellation point at each layer. However, they all fall short in terms of complexity or performance, which leads to two proposed solutions to mitigate EVS.

1.4 Thesis Organization

This thesis is organized as follows: Previous work and proposed time domain QR-RLS chan-

nel estimator are described in detail in chapter two. Since all simulation parameters use Wimax (802.16m) standard phy. layer, an overview of Wimax system block diagram and down link frame format is given in chapter three. The fourth chapter describes joint coarse-fine QR-LS channel estimator for fast fading channel environment. Soft output generation and EVS (Empty Vector Set) problem for SM-MIMO data detection is defined in the fifth chapter. The sixth chapter provides two different solutions to mitigate EVS problem and produce soft output. The thesis is concluded in chapter seven.

Chapter 2

QR-RLS based MIMO-OFDM Channel Estimator

2.1 Channel Estimation in OFDM Systems

Generally, in OFDM system (for ex. Fig.(3.1)), the transmitter modulates the message bit sequence into PSK/QAM symbols, performs IFFT on the symbols to convert them into time domain signals and sends them out through a channel. The received signal undergoes multi-path and additive noise effect while propagating through wireless medium. The channel effect is estimated and compensated in the receiver to recover original transmitted bits sequence. When the received signal is free from ICI[66], orthogonality between subcarriers is maintained. This in turn allows each subcarrier component of the received signal to be expressed as the product of the transmitted signal and channel frequency response at the subcarrier. Thus, the transmitted signal can be recovered by estimating the channel response just at each subcarrier.

In general, the channel can be estimated by using a preamble or pilot symbols known to both transmitter and receiver, which employ various interpolation techniques to estimate the channel response of the subcarriers between pilot tones. In several techniques[51][20][13], channel is estimated in time domain using inherent correlations of received signal by adaptive methods and then transformed to frequency domain as channel response of the subcarriers. In order to choose the channel estimation technique for the OFDM system under consideration, many different aspects of implementation, including the required performance, computational complexity and time-variation of the channel must be taken into account.

2.2 Time Domain Channel Estimation

2.2.1 Previous Work

As discussed earlier, depending on the requirement various channel estimation methods are considered by literature. Author[31] proposed that OFDM, a wireless access method is much more robust for multipath channel impairments compared to FDMA, TDMA. Generally it uses orthogonal tones for data transmission and thus prevents any guard band requirements between two consecutive tones. In[11], the author exploits (MIMO) multiple antenna technology by processing spatial dimension to gain more capacity as well as diversity compared to single antenna systems. Combining the two technologies mentioned above, results in MIMO-OFDM[44] system, which in turn results in a very promising system with capacity increase and robustness to channel impairments.

Author[63][35] proposed the use of DPSK modulation scheme to successfully decode the received signal without channel knowledge. Author[63] mentioned the need for channel estimation to use multi amplitude modulation scheme for coherent detection. He mentioned MMSE, LSE estimator. However, MMSE estimator being computationally complex also requires prior knowledge of channel statistics. He simplified MMSE estimator by truncating the low energy values of autocorrelation matrix to zero which results in modified MMSE estimator. He also mentioned the use of just a scalar division which results in LS estimation in frequency domain. Author[8] proposes the use of SVD decomposition for LMMSE estimator which results in low rank estimator while preserving the performance.

Author[35] suggested robust MMSE channel estimator which overcomes pre-requirement of channel statistics by fully utilizing time and frequency correlations of the frequency response of time varying dispersive fading channels. Author[2] [36] suggested optimal training sequence based simplified channel estimator for MIMO-OFDM system. In this method, training sequence is designed by carefully selecting the relative phase of training sequences between different transmitting antennas. In [18] the author proposed two one-dimensional separable wiener filters for frequency selective channels. Here he assumes the worst channel parameter statistics like maximum Doppler spread and maximum Delay spread to approximate autocorrelation matrix.

Using above idea author[55] proposes adaptive wiener filter for time varying channels which do not require prior knowledge of channel statistics. However, he uses NLMS and RLS algorithm to update wiener filter coefficients. In[20], the author proposed adaptive RLS based channel estimator for OFDM systems, which eliminates the need for channel correlations. Author[27] has shown the use of Decision Directed Channel Estimation(DDCE) joint channel tracking and data estimation for MIMO block fading channels. In such a case, channel tracking is done during train-

ing period and then the data is detected using channel knowledge. In[51], the author shows that time domain method exploits the inherent frequency correlation among the taps. Hence it is more robust compared to frequency domain estimation[63] where the estimation error will get spread over the whole frequency band. In[52], the author suggested adaptive RLS channel estimator for MIMO extended WLAN. Generally, RLS based estimators involve matrix inversion which leads to high computational complexity and produces round-off error. In [39], the author showed the effect of round-off error and also[9][14] suggested use of square root(QR) estimators to mitigate round-off error.

In continuation to the work referred to above, here, preamble based QR-RLS adaptive[48] channel estimator for MIMO-OFDM systems is derived. The proposed algorithm is a linear extension of its SISO version given in [47]. The proposed estimator uses QR factorization of correlation matrix[38] and thus simply avoids complexity and round-off error. Here, the major focus has been on complexity reduction from $O(N^3)$ to $O(N^2)$ and ease of updating QR estimator for time varying channels. Estimated channel at preamble symbol is then used for data detection with two different modes. For flat fade channel, first order Markov process is applied for estimating channel fading parameter. This in turn uses DD(Decision Direct) mode for data detection for the rest of the frame. However, for fast fading channels, further performance improvement can be achieved by joint preamble-pilot based channel estimation and is described in a later chapter.

2.3 MIMO System Model

A general MIMO system model with N_t transmit, N_r receive antennas is shown in Fig.(2.1). $X_1, X_2, X_3....X_{Nt}$ represents respective input signals to N_t input antennas, where

$$X_p = [x_{(p,n)}, x_{(p,n+1)}, ...x_{(p,n+Ns-1)}]$$

at time n, with Ns data symbols. For making analysis simple consider $Nt = Nr$.

The Multipath time variant channel between p^{th} transmit and q^{th} receive antenna with L resolvable paths is given by

$$h_{pq}(\tau, t) = \sum_{n=0}^{L-1} \beta_{pq}(l) \cdot \delta(\tau - \mathcal{T}_l) \tag{2.1}$$

where

$$\beta_{pq}(l) = \alpha_{pq}(l) \cdot e^{j(\theta_l + 2\pi f_{(D,l)} t)} \tag{2.2}$$

where α_l, θ_l and $f_{(D,l)}$ denote the amplitude, phase and the Doppler shift of the lth path, respectively.

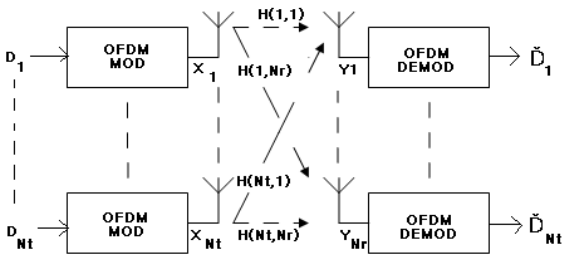

Figure 2.1: MIMO OFDM System Model

Assuming isotropic scattering, the autocorrelation of the path gains as shown in[64] is

$$r_l(\tau) = E[\beta_l^*(t)\beta_l(t+\tau)] = \sigma_l^2 J_0(2\pi f_{Dmax}\tau) \tag{2.3}$$

where σ_l^2 is the power of the lth path gain, $J_0(x)$ is the Bessel function of the first kind of order 0, and f_{Dmax} is the maximum Doppler frequency which is related to the velocity v of movement and the wavelength λ of the carrier frequency $f_{Dmax} = v/\lambda$.

The received signal Y at time n, in square matrix form having dimension $[(Nt \cdot L) \times (Nt \cdot L)]$ can be expressed as

$$Y(n) = (U(n) \cdot H(n)) + V(n) \tag{2.4}$$

where matrix $U(n)$ is prewindowed matrix[38] of $[(Nt \cdot L) \times (Nt \cdot L)]$ having $Nt \cdot L$ data symbols from each Tx. antenna at time instant n, For ex. at time instant n = 0, $U(0)$ is given by,

$$\begin{pmatrix}
x_{1,0} & 0 & . & 0 & . & x_{Nt,0} & 0 & . & 0 \\
x_{1,1} & x_{1,0} & . & 0 & . & x_{Nt,1} & x_{Nt,0} & . & 0 \\
. & . & . & . & . & . & . & . & . \\
x_{1,L-1} & x_{1,L-2} & . & x_{1,0} & . & x_{Nt,L-1} & . & . & x_{Nt,0} \\
. & . & . & . & . & . & . & . & . \\
x_{1,2L-1} & . & . & x_{1,L} & . & x_{Nt,2L-1} & . & . & x_{Nt,L} \\
. & . & . & . & . & . & . & . & . \\
. & . & . & . & . & . & . & . & . \\
x_{1,Nt\cdot L-1} & . & . & . & . & . & . & . & x_{Nt,L}
\end{pmatrix}$$

where rows of matrix U represents prewindowed data, like prewindowed data at time n is

$$Xpre(n) = [x_{1,n}, x_{1,n-1}, ..x_{1,n-L+1}, x_{2,n}, x_{2,n-1}..., x_{Nt,n}...]$$

$Y(n)$ is $[(Nt \cdot L) \times (Nt \cdot L)]$

$$Y(n) = [Y_1(n), Y_2(n), Y_3(n)...Y_{Nr}(n)]$$

where $Y_q(n)$ is

$$Y_q(n) = [y_{(q,n)}, y_{(q,n+1)}...y_{(q,n+(Nr \cdot L)-1)}]^T$$

and

$$H(n) = [H_1(n), H_2(n), ...H_{Nr}(n)]$$

where $H_q(n)$ is

$$H_q(n) = [H_{(1,q)}(n), H_{(2,q)}(n)...H_{(Nt,q)}(n)]^T$$

and $H_{(p,q)}(n)$ is

$$H_{(p,q)}(n) = [h_{pq}(n,0), h_{pq}(n,1), ...h_{pq}(n,L-1)]^T$$

V is $[(Nt \cdot L) \times (Nt \cdot L)]$with complex elements that are independent and identically distributed(i.i.d.) Gaussian random variable with zero mean and variance σ_v^2.

2.4 Proposed QR-RLS based Coarse Channel Estimation using Preamble

Each transmitter transmits Preamble as first OFDM symbol. Channel is estimated during this training period, where estimated channel is $\bar{H}$.

Consider the received signal at q^{th} receive antenna represented in matrix form as

$$Y_q(n) = (U(n) \cdot H_q(n)) + V_q(n) \tag{2.5}$$

The posteriori error is given by the difference between the received preamble symbol and it's corresponding estimate at time n on q^{th} receiving antenna

$$e(q,n) = y(q,n) - \bar{y}(q,n) \tag{2.6}$$

$$e(q,n) = y(q,n) - Xpre(n).\bar{H}_q \tag{2.7}$$

Where $\bar{H}$ has the same dimensionality as H. The Weighted Least square error at time n is given by

$$\zeta(n) = \sum_{i=0}^{n} \lambda^{n-i} |e(q,i)|^2, \tag{2.8}$$

where λ is forgetting factor, whose value lies between (0,1) depending on channel fading conditions. Solution of the above equation gives the optimum value for the estimated channel coefficients H at time n. The optimum solution of Eq.(2.8) is given by[14][37]

$$\bar{H}_q(n) = R_X^{-1}(n) \cdot R_{Y_q X}(n) \tag{2.9}$$

where $R_X = (U^T U) = X_{pre}^T X_{pre}$ is the autocorrelation matrix of the preamble signal, and $R_{Y_q X}$ is the cross correlation matrix between received signal and the preamble signal at time n.

Using simplicity, by rewriting above Eq.(2.9)

$$\bar{H}_q(n) = \left(X_{pre}^T(n) X_{pre}(n)\right)^{-1} X_{pre}^T Y_q(n) \tag{2.10}$$

Initialization: Decomposition of matrix U is given by

$$U_{(Nt\cdot L)\times(Nt\cdot L)} = Q_{(Nt\cdot L)\times(Nt\cdot L)} R_{(Nt\cdot L)\times(Nt\cdot L)}$$

Where Q is orthogonal matrix and R is upper triangle matrix. substituting this into Eq.(2.10) results in

$$\bar{H}_q(n) = R^{-1}(n) Q^T Y_q(n) \tag{2.11}$$

Each antenna has it's own preamble sequence.

Updating: QR decomposition of compound matrix U at time n is

$$[U(n)|Y_q(n)]_{(Nt\cdot L)\times((Nt\cdot L)+1)} = S(n).T(n) \tag{2.12}$$

where

$$S(n) = [Q(n)|q(n)]_{Nt\cdot L)\times(Nt\cdot L)+1)}$$

and

$$T(n) = \left[\frac{R(n)|Z(n)}{0|\xi(n)}\right]_{(Nt\cdot L)+1)\times(Nt\cdot L)+1)}$$

where $Z(n) = R_{Y_q X}(n) = Q^T d(n)$ from Eq.(2.12). Then at time $(n+1)$

$$[U(n+1)|D(n+1)]_{(Nt\cdot L)+1)\times(Nt\cdot L)+1)} = S(n+1).T(n+1) \tag{2.13}$$

$$T(n+1) = [Q(n+1)|q(n+1)]_{(Nt\cdot L)+1)\times(Nt\cdot L)+1)}$$

$$S(n+1) = [\frac{R(n+1)|Z(n+1)}{0|\xi(n+1)}]_{(Nt\cdot L)+1)\times(Nt\cdot L)+1)}$$

where updated matrix using Eq.(2.12) and Eq.(2.13) is

$$[U(n+1)|D(n+1)] = [\frac{U(n)|D(n)}{X(n+1)|d(n+1)}] \tag{2.14}$$

combining Eq.(2.12)(2.13) and(2.14) and keeping the fact that last row of R is 0, the new matrix for QR factorization at time $(n+1)$ is

$$[U(n+1)|D(n+1)] = [\frac{R(n)|Z(n)}{X(n+1)|d(n+1)}] \tag{2.15}$$

by QR factorizing above Eq.(2.15) updated vector

$$\bar{H}_q(n+1) = R_x^{-1}(n+1)Z(n+1) \tag{2.16}$$

is computed.

2.5 DD Mode for Data Detection

As shown above, let $H_q(n)$ is channel estimated at time n. Assuming that the CIR taps are slowly varying and fade at the same Doppler rate, then it may be possible to statistically describe such variations according to the first order Markov process as follows [13]

$$H_q(n+1) = A \cdot H_q(n) + V_q(n) \tag{2.17}$$

where $A = aI$
and $a = J_0(2\pi \cdot f_{D_{max}} \cdot T_s)$
The above term is a parameter very close to unity and it indicates that channel variation is minor from time n to n+1. Channel is estimated using this assumption for the rest of the frame (symbols other than preamble). However, in fast fading channel the above mentioned Markov model based

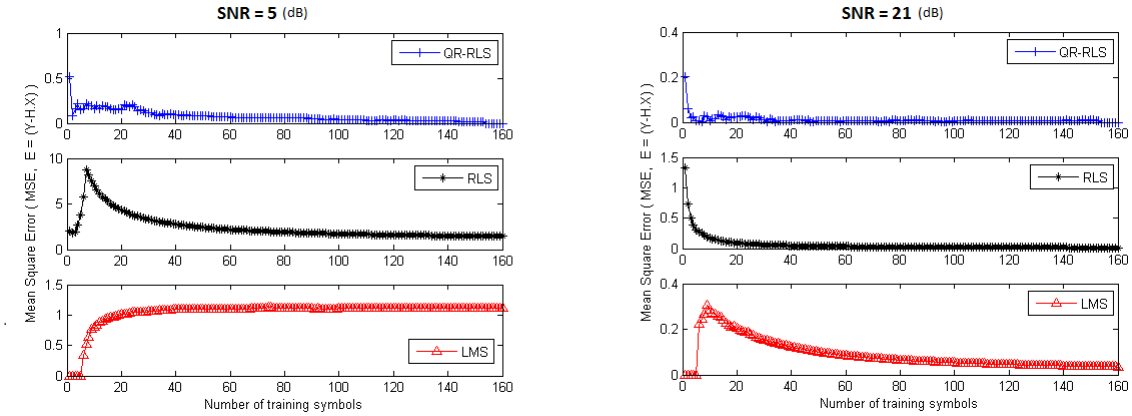

Figure 2.2: Convergence of Various Methods

estimation is not very useful. In such case, scattered pilots provide the additional information regarding channel variation which helps in performance improvement as shown in a later chapter.

2.6 Simulation Results

SISO System Parameters Simulation parameters:
Frame size : 2 subframes
OFDM symbols per subframe : 5
First Symbol of each frame is Preamble symbol
Preamble length : 160 samples
FFT size: 64
CP size : 16
Fs = 11.2 MHz
Ts = 112 μsec
Channel profile: Flat fade channel with channel length L = 6, 29
Doppler Frequency FDmax $\leq$ 5
No. of Tx and Rx. antenna = 1
Forgetting factor λ for RLS, QR-RLS = (0.995 $\rightarrow$ 1)

The above Fig.(2.2) shows the convergence results for various channel estimators at two different SNR values. The channel considered here is flat fade channel with channel length L = 6. The graph shows that proposed estimator only uses $\leq$ 10 percent of training data and at the same time results in faster convergence to optimum solution compared to other methods. Result also shows

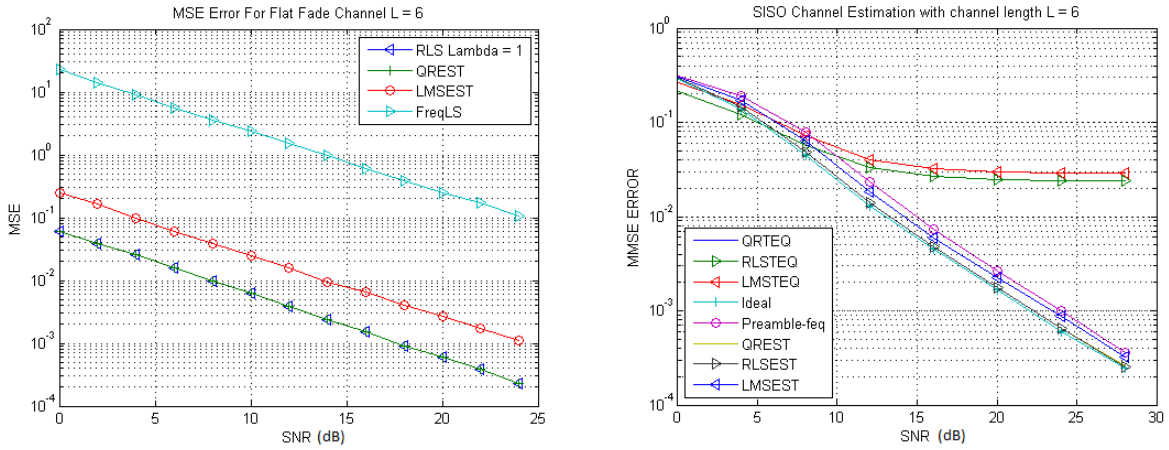

Figure 2.3: Channel Estimation Error and BER performance for Various Estimators

that RLS estimator and proposed QR-RLS estimator provides similar performance for forgetting factor 1, except less computational complexity for the propsed one.

The simulation result in Fig.(2.3) compress various channel estimation and TEQ methods to overcome channel fading effects. Comparision is provided for flat fade channels with different channel lengths. The performance is evaluated in terms of MSE error of channel estimate, which is defined as $e(n) = E \parallel H(n) - \bar{H}(n) \parallel^2$. Comparison is between MMSE[63][35], LMS based TEQ[29], RLS, QR-RLS based TEQ[47], RLS[20],QR-RLS based Channel estimation, Frequency domain LS[63] estimation. For flat fade channel, forgetting factor is kept 1, which results in overlap of RLS, QR-RLS estimator MSE, BER curves and can be seen in Fig.(2.3). Also, Fig.(2.3),(2.4) clearly indicates that for flat fading channels with (CIR $\leq$ CP) almost every estimator works well. MMSE gives superior performance while frequency domain LS gives quite inferior performance at the advantage of lowest complexity. LMS, RLS based inverse ZF TEQ results in inferior perfomance due to noise amplification and it get worsen for CIR $>$ CP. Fig.(2.4) shows BER performance results for the case (CIR $\geq$ CP), In such case, estimator with lower filter taps doesn't reach the near optimum performance. However, increasing the number of taps according to channel rank($\approx$ channel length L), near optimum performance results can be gained.

MIMO System Parameters

Simulation parameters:

Frame size : 2 subframes

OFDM symbols per subframe : 5

First Symbol of each subframe is Preamble symbol

FFT size: 1024/2048

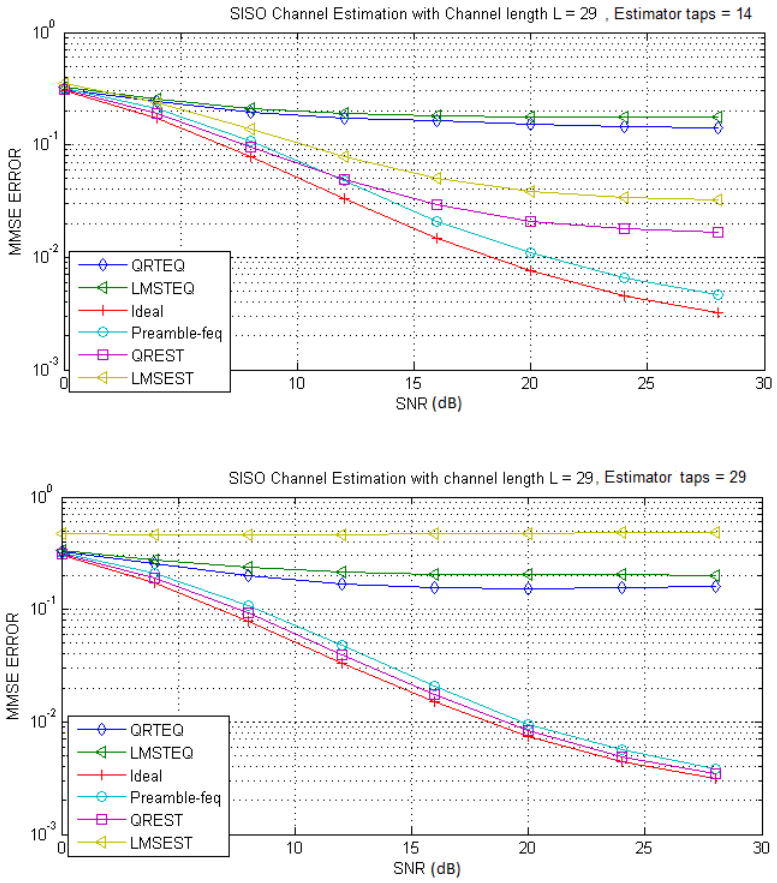

Figure 2.4: BER Performance for Estimator with 14 taps and 29 taps

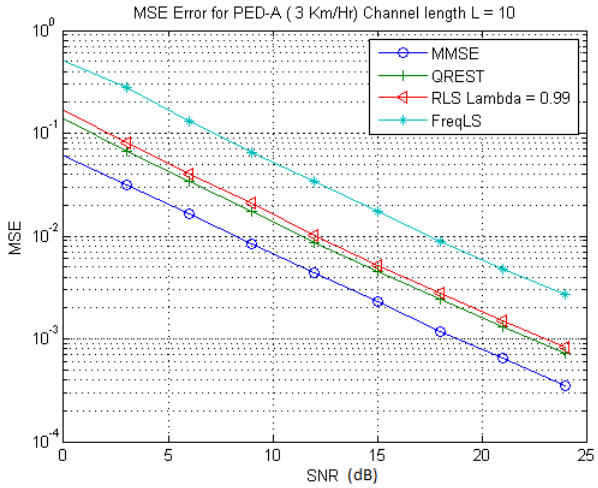

Figure 2.5: Comaprision of Chanel Estimation Error For 2x2 MIMO system

Fs = 11.2/22.4 MHz
Ts = 103.5 μsec
Channel profile: PED-A (3-30 km/hr), Veh-A (30-120 km/hr)
Doppler Frequency FDmax = 8-300
No. of Tx and Rx. antenna = 2
Forgetting factor λ for RLS, QR-RLS = $(0.99 \rightarrow 1)$

Here the number of subcarriers is increased from 64 to 1024/2048, which helps in dividing the channel bandwidth into more parts and makes frequency selectivity to almost flat one. The number of antennas is also increased in spatial direction to achieve more throuhput. However it comes with additional channel estimation requirements (for the considered case, 4 channel should be estimated) compared to SISO case. Fig(2.5) compares MSE error for all channel estimators for 2x2 MIMO systems. Since channel is realized for 1000 realizations with diffrent vehicular speeds varying from 3km/hr to 120 km/hr, the forgetting factor ranges from $(0.99) \rightarrow 1$. Simulation result of Fig. (2.5) almost follows the SISO channel estimation results. Fig.(2.6) shows convergence results of propesed estimator for MIMO-OFDM system with different SNR values. Fig.(2.7),(2.8) compare MSE error and BER performances of the proposed estimator with various estimators for 2x2 MIMO systems. As discussed earlier, orthogonal preamble sequence is used for two antenna system. BER performance can be found by DDCE method. For Ped-A channel, channel variations are slow which results in fading parameter almost equal to 1 and can be well approximated by the method used. However, for Veh-A channel the MSE, BER gap increases between ideal channel

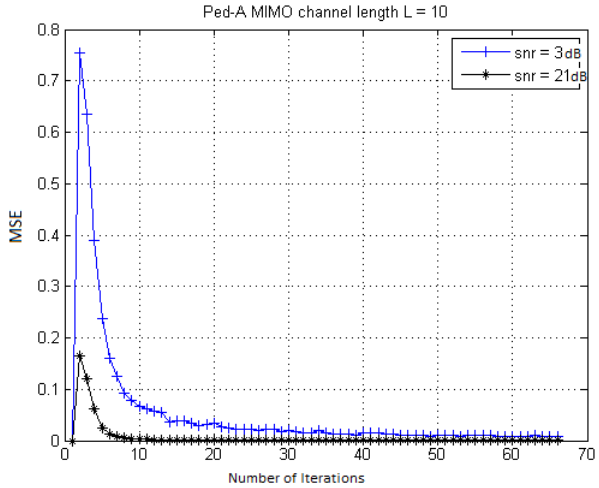

Figure 2.6: QR-RLS Estimator Convergence for Different SNR

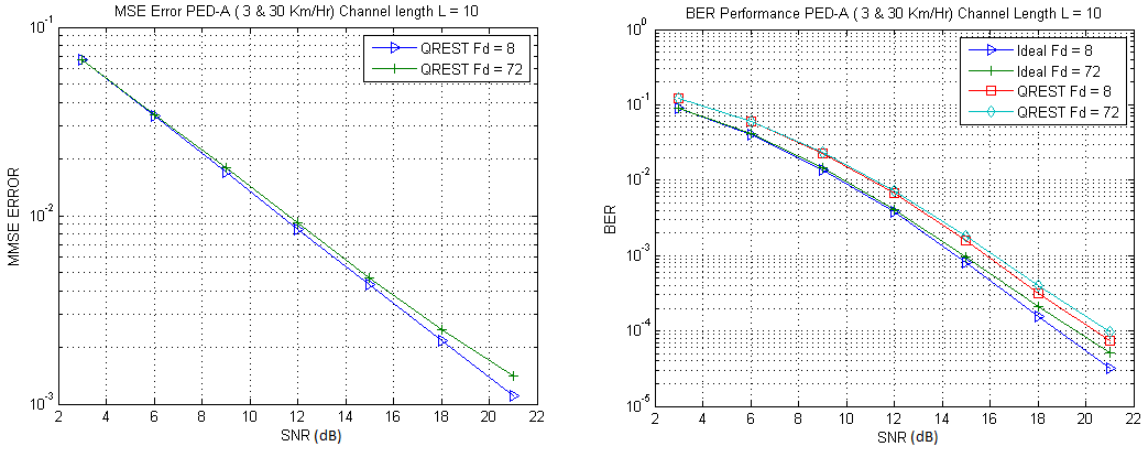

Figure 2.7: MSE Error and BER performance for PED-A channel With Different speeds

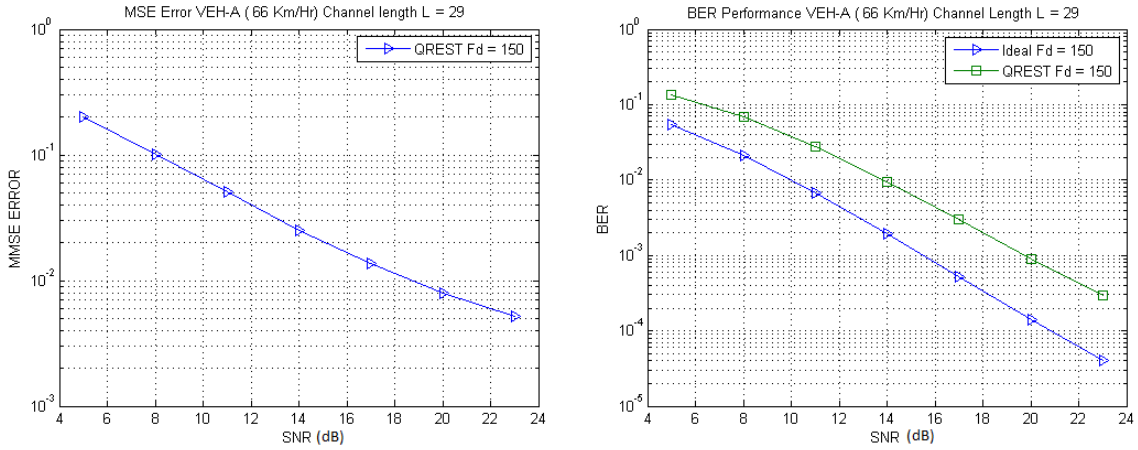

Figure 2.8: MSE Error and BER performance for VEH-A channel

Table 2.1: Complexity of All Adaptive Time Tracking Methods[47]

Method	Complexity in Complex multiplications (channel length P)
LMS	$2P$
RLS	$3(P^2+2P+2)$
$QR-RLS(Gram-schmidt)$	$3(P-1)^2+2p^2$
$QR-RLS(GivensRotation)$	P^2+5p

known and proposed estimator. The increase in error gap for BER peformane is due to the assumption of fading rate according to Markov model. This shows that performance results get worse for fast fading channel.

Chapter 3

Wimax Overview

Wimax Phy. Layer is based on orthogonal frequency division multiplexing(OFDM). OFDM is the transmission scheme of choice to enable high-speed data, video and multimedia communications and is used by a variety of commercial broadband systems, including DSL, Wi-Fi, Digital Video Broadcast-Hand held (DVB-H) and WiMAX. Also, OFDM is an efficient scheme for high data rate transmission in a non-line-of-sight(NLOS) or multipath radio environment.

3.1 Wimax: An Example of MIMO-OFDM System

3.1.1 Transmitter

Block Diagram in Fig.(3.1) shows various functional stages of a Wimax Phy. Layer. As a specific case DownLink Transceiver of 802.16m is considered here. It consists of a Channel Encoder, QAM Mapper, MIMO Mapper, Resource allocation, Carrier mapping by IFFT and (Cyclic Prefix) CP addition block (to prevent ISI). A brief description of each block is given below.

Channel Coding

Channel coding stage consists of the following steps: (1) data randomization, (2) channel coding, (3) rate matching, (4) HARQ, if used and (5) interleaving.
Data randomization is performed in the uplink and the downlink, using the output of a maximum length shift-register sequence that is initialized at the beginning of every FEC block. The purpose of the randomization stage is to provide layer 1 encryption and to prevent a rogue receiver from decoding the data. Channel coding is performed on each FEC block which adds redundancy in the code. By means of rate matching, any arbitrary code rate can be achieved from a fixed-rate mother

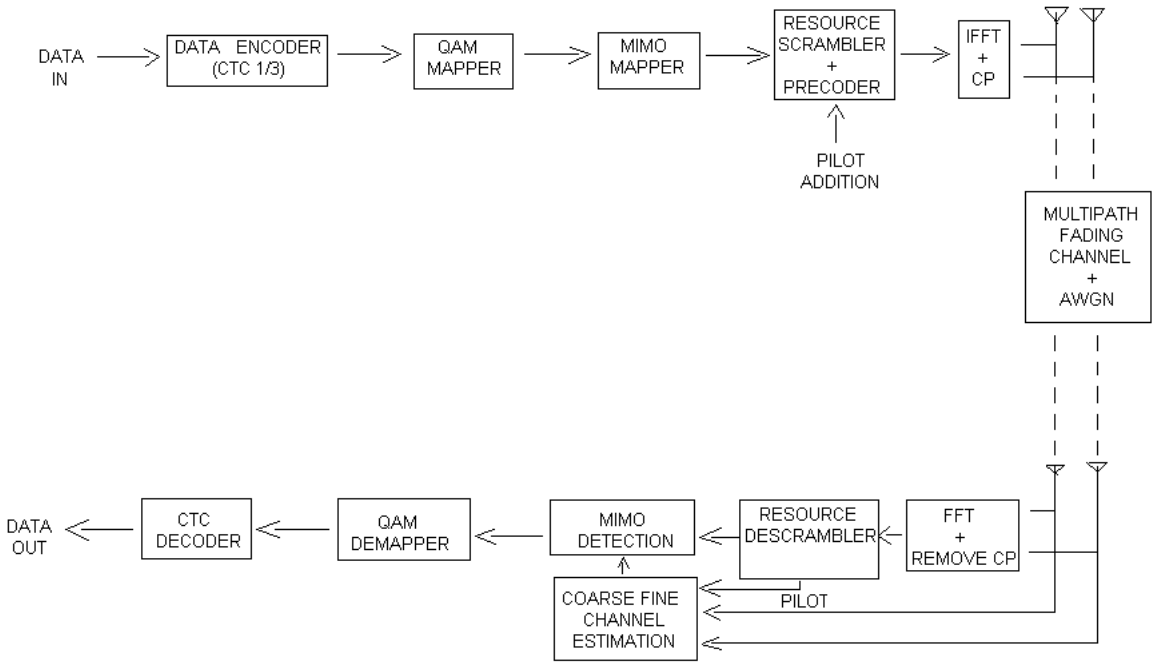

Figure 3.1: Block Diagram DL Tx 80216m

code. Any code rate (r) can be obtained from the initial $1/3$ code via a process of bit puncturing for $(r \geq (1/3))$ or repetition $(r \leq (1/3))$. Interleaving helps to provide maximum decorrelation between two Turbo encoded data sequences. This helps during channel fades as both sequences cannot be similarly affected. Generally, Turbo codes are used for channel encoder due to their better convergence, greater minimum distances between generated codewords, less sensitivity to puncturing patterns and robustness of the decoder[59][56].

QAM-Mapper

The sequence of binary bits is converted to a sequence of complex valued symbols. The constellations are QPSK and 16 QAM, 64 QAM constellation. Each modulation constellation is scaled by a number c, such that the average transmitted power is unity. The value of c is $\sqrt{1/2}$, $\sqrt{1/10}$ and $\sqrt{1/42}$ for the QPSK, 16 QAM, and 64 QAM modulations, respectively.

MIMO Mapper

There are various MIMO open loop and close loop modes with transmit and receive diversity as explained earlier. Here, the work consider only SM case in particular with SU-MIMO (Single

User-MIMO) case to achieve high throughput.
MIMO Mapper is made of MIMO encoder and MIMO precoder. MIMO encoder maps input MIMO layers to MIMO streams. MIMO layer is an information path fed to the MIMO encoder as an input. For example, in SFBC encoding, the input data $s = [s_1, s_2, s_3....]$ to MIMO encoder is divided in pairs of consecutive 2×1 sample pairs (MIMO layer). The first pair is

$$\begin{pmatrix} s_1 \\ s_2 \end{pmatrix}$$

MIMO encoder encodes

$$\begin{pmatrix} s_1 & -s_2^* \\ s_1^* & s_2 \end{pmatrix}$$

Since here SM case with 4×4 antenna is considered, MIMO stream mapping (Vertical encoding) is

$$\begin{pmatrix} s_1 \\ s_2 \\ s_3 \\ s_4 \end{pmatrix}$$

MIMO precoder uses a set of codebooks to map MIMO stream to antenna. The output of the MIMO encoder is multiplied by a precoder weight matrix W. The Matrix from the codebook is chosen according to some fixed statistics in open loop and channel feedback knowledge in closed loop. Precoder is much more useful for directional beamforming when multiuser MIMO is used. It helps to nullify or minimize interference for a selected user due to other users' data transmission.

Resource Mapper

According to channel conditions, the data is allocated to available resource subchannels. A subchannel is a group of subcarriers (orthogonal frequencies in this case). Under good channel conditions, large band of adjacent subcarriers are assigned. However, under worst conditions, adjacent data is assigned to permuted subcarriers, so that the resultant signal doesn't experience a continuous deep fade. Pilots are added in the resultant block signal while fulfilling the delay spread and coherence time spacing in time-frequency subframe grid to carry out channel estimation at the receiver.

IFFT

It assigns orthogonal frequencies (OFDM as explained earlier) to MIMO data streams from MIMO Mapper block.

Wireless Channels

Data is transmitted by multiple antennas and propagates through multipath fading channel with additive noise as explained earlier.

3.1.2 Receiver

Channel Estimation

This block is responsible for tracking the channel multipath effect and time variation and is described in detail in a later chapter. The first block in the receiver is the channel estimator. The need for channel estimation has been explained earlier. Previous work for SISO/MIMO channel estimation, Block/Comb pilot interpolation based Slow-Fast fading channel estimation, Wimax channel estimation requirements and proposed joint Coarse-Fine channel estimation methods is detailed in other chapters.

MIMO Hard/Soft Detection

Once the channel is estimated, then MIMO data streams are detected using various MIMO linear and OSIC detectors. Soft QR-OSIC based detectors are optimal in terms of performance and complexity, but they suffer from EVS (Empty Vector Set) problem. The appropriate solution while achieving soft ML capacity is described in detail in a later chapter.

CTC Decoder

The decoder is iterative Turbo decoder and uses Max log Map, BCJR algorithm[3][56]. The decoder uses 3-4 internal iterations and exchanges soft information between two internal decoders back and forth to achieve extrinsic gain. Usefulness of extrinsic gain in achieving soft ML capacity is explained in a later chapter. The other blocks like MIMO demapper, QAM demapper are dual of transmitter blocks.

3.2 Wimax Frame Format

As shown in Table 775 of [23], various OFDMA parameters are considered for different channel bandwidths. Here the work concentrate on one particular case with parameters as shown in Fig.(3.2).

The nominal channel bandwidth, BW (MHz)			10	20
Sampling factor, n			28/25	28/25
Sampling frequency, F_s (MHz)			11.2	22.4
FFT size, N_{FFT}			1024	2048
Subcarrier spacing, Δf (kHz)			10.94	10.94
Useful symbol time, T_b (μs)			91.4	91.4
CP ratio, $G = 1/8$	OFDMA symbol time, T_s (μs)		102.857	102.857
	FDD	Number of OFDMA symbols per 5ms frame	48	48
		Idle time (μs)	62.857	62.857
	TDD	Number of OFDMA symbols per 5ms frame	47	47
		TTG + RTG (μs)	165.714	165.714

Figure 3.2: OFDMA parameters for Considered Case

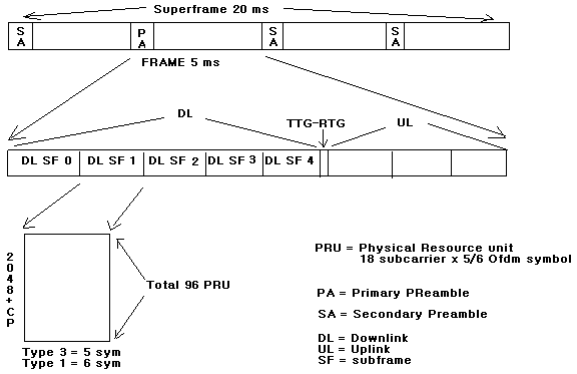

Figure 3.3: WiMax Basic Frame Structure

The advanced air interface basic frame structure is illustrated in Fig (3.3). Each 20 ms superframe is divided into four equally-sized 5 ms radio frames. When using the same OFDMA parameters with the channel bandwidth of 20 MHz, each 5 ms radio frame further consists of eight AAI subframes for G = 1/8. An AAI subframe shall be assigned for either DL (Down Link) or UL (Up Link) transmission. Two types of AAI subframes are considered:

1) The type-1 AAI subframe which consists of six OFDMA symbols,

2) The type-3 AAI subframe which consists of five OFDMA symbols.

The basic frame structure is TDD duplexing. The number of switching points in each radio frame is two, where a switching point is defined as a change of directionality, i.e., from DL to UL or from UL to DL.

3.2.1 TDD Frame Structure

In a TDD frame with DL to UL ratio of D:U (Down Link to Up Link), the first contiguous D AAI subframes and the remaining U AAI subframes are assigned for DL and UL respectively, where $D + U = 8$ for 20 MHz channel bandwidths. TTG (Transmit Transition Gap) and RTG (Receive Transition Gap) are 105.714 μs and 60 μs, respectively.

Downlink Physical Structure [23]

Each down link AAI subframe is divided into 4 or fewer frequency partitions. Each partition consists of a set of physical resource units across the total number of OFDMA symbols available in the AAI subframe. Each frequency partition can include contiguous (localized) and/or non-contiguous (distributed) physical resource units.

Physical and Logical Resource Unit

A PRU (Physical Resource Unit) is the basic physical unit for resource allocation that comprises Nsc consecutive subcarriers by Nsym consecutive OFDMA symbols. Nsc is 18 subcarriers and Nsym is 6 and 5 OFDMA symbols for type-1 and type-3 AAI subframes respectively. A LRU (Logical Resource Unit) is the basic logical unit for distributed and localized resource allocations. An LRU is Nsc·Nsym subcarriers for type-1 AAI subframes, type-3 AAI subframes. The effective number of subcarriers in an LRU depends on the number of allocated pilots. Fig. (3.4) describes various resorce units.

Distributed Logical Resource Unit

The DLRU (Distributed Logical Resource Unit) consists of a group of subcarriers that are spread across the distributed resource allocations within a frequency partition. The size of the DLRU equals the size of PRU, i.e., Nsc subcarriers by Nsym OFDMA symbols. The minimum unit for forming the DLRU is equal to a pair of subcarriers called a tone-pair. The DLRUs are obtained by subcarrier permutation of the DRUs (Distributed Resource Units).

Contiguous Logical Resource Unit

The localized logical resource unit, also known as CLRU (Contiguous Logical Resource Unit) contains a group of subcarriers that are contiguous across the localized resource allocations. The size of the CLRU equals the size of the PRU, i.e., Nsc subcarriers by Nsym OFDMA symbols. The

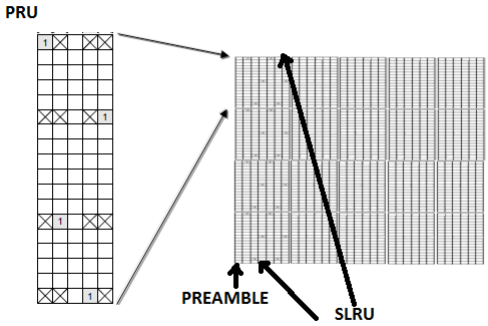

Figure 3.4: Resource Unit

CLRUs are obtained from direct mapping of Contiguous Resource Units (CRUs). Two types of CLRUs, Subband LRU (SLRU) and Miniband LRU (NLRU), are supported respectively. Here the work concentrate on Subband CRUs only.

Subband vs. Miniband

The PRUs are first subdivided into subbands and minibands. A subband comprises of N1 adjacent PRUs and a miniband comprises of N2 adjacent PRUs, where N1 = 4 and N2 = 1. Subbands are suitable for frequency selective allocations as they provide a contiguous allocation of PRUs in frequency. Minibands are suitable for frequency diverse allocation and are permuted in frequency.

Pilot Structure

The transmission of pilot subcarriers in the down link is necessary for enabling channel estimation, measurement of channel quality indicators such as the SINR, frequency offset estimation, etc. The pilot patterns on stream 0 - stream 3 for four pilot streams are shown in Fig. (3.5).

Advanced Preamble

There are two types of Advanced Preamble (A-Preamble): Primary Advanced Preamble (PA-Preamble) and Secondary Advanced Preamble (SA-Preamble). One PA-Preamble symbol and three SA-Preamble symbols exist within the superframe. The location of the A-Preamble symbol is specified as the first symbol of the frame. SA-Preamble for 2048 FFT, 4 antenna case is shown in Fig. (3.6), which shows that generated preamble sequence for four antennas are orthogonal and do not contribute interference to each other. Here, the work utilizes SA-Preamble to estimate channel

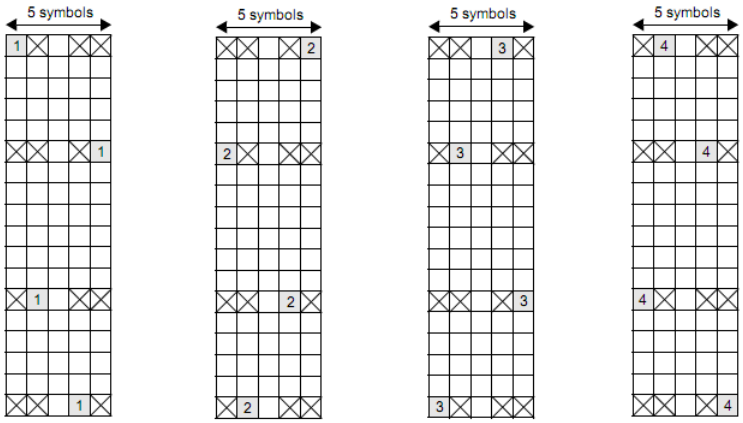

Figure 3.5: Pilot Pattern for 4 data streams

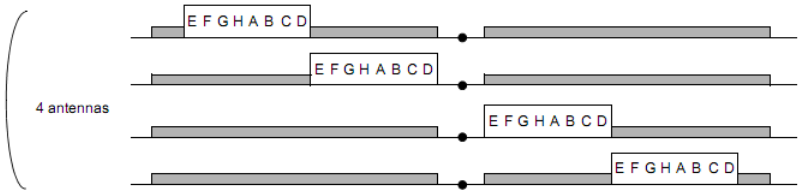

Figure 3.6: SA-Preamble

in time domain using QR-RLS estimator.

As seen in the frame format, preamble is followed by subframe zero. It consists of SFH (Super Frame Header), A-MAP and data burst. SFH contains control data information like, frequency offset, OFDM symbol number for data burst start and end, number of users, number of CRUs/DRUs allocated etc. Subframe 1 and 2 follow subframe 0, which consists of data bursts allocated in different frequency partitions. MIMO midamble then follows which is used for Channel Quality Information (CQI) during MIMO close loop configuration. CQI estimated at mobile station using MIMO midamble is then fed back for codebook selection when used in MU-MIMO environment. Subframe 4 and 5 contain data burst which is follwed by TTG and UL data.

Chapter 4

QR-LS Based Coarse-Fine Channel Estimator

4.1 Pilot Based Estimation

4.1.1 Previous Work

Generally OFDM system performance is greatly influenced by channel estimation. Pilot symbol assisted channel estimation is one of the promising methods due to its simple implementation and robust performance. Author [63] suggested block pilot (training data) based MMSE, LSE estimator for OFDM systems. Author [19] derived 2D optimum wiener filter for pilot based channel estimator. The author in [34] proposed pilot assisted robust channel MMSE estimator for OFDM systems which doesn't require prior knowledge of channel statistics. Author [62] proposed a novel pilot based estimation (with different pilot patterns) depending on channel statistics that leads to better BER performance or reduced number of pilots. Author [67] represented a transform domain DFT-IDFT technique using pilots for channel estimation.

In [21][6] the author suggested Block, COMB pilot arrangement [4] for channel estimation in OFDM systems. He has shown that in block type, OFDM symbols with pilots at all subcarriers (carriers in frequency direction of Time-Freq. grid) are transmitted periodically for channel estimation. A pilot at each subcarrier leads to better channel estimation for frequency selective channels. At the same time, periodic transmission with period of coherence time will keep good track of time-varying channel characteristics. Similarly COMB type pilot arrangement is good for fast fading channel. In [4] [19] the author used scattered pilot arrangement for channel estimation. In this method, pilots are scattered with period of coherence time and coherence bandwidth in time and

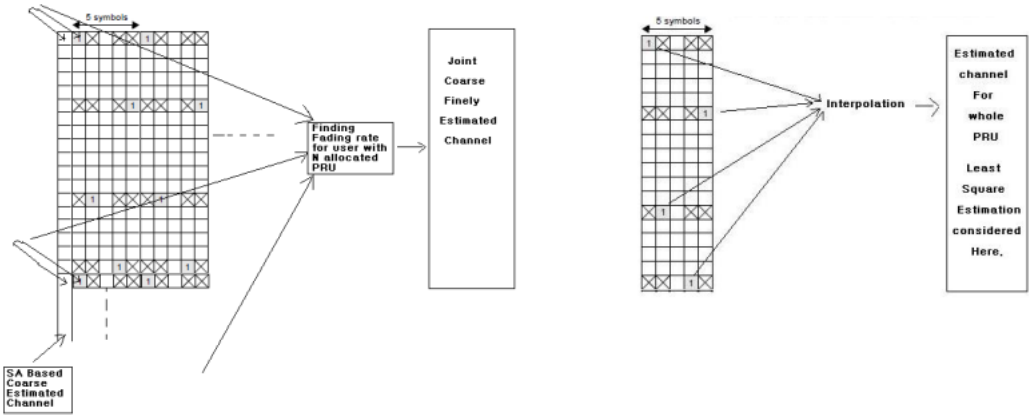

Figure 4.1: Preamble-Pilot based Coarse-Fine Vs. COMB Pilot Based Linear Estimation

frequency direction of Time-Freq. grid respectively. Such an arrangement leads to better channel tracking for frequency selective as well as fast fading channel environment.

Generally, various interpolation methods MMSE [34][7][67][61] are used along with scattered pilots to estimate channel at every point. Author [7] represented a report on linear interpolation based pilot assisted channel estimator. However, all the work mentioned above use pilots in frequency domain for channel estimation which itself is inferior to its time domain counterpart for OFDM systems [51]. In the presented work, performance improvement over pilot based estimator is gained using time-frequency joint channel estimator as discussed below.

4.2 Proposed QR-LS Coarse-Fine Channel Estimation for WiMax

4.2.1 Background

As discussed earlier, DDCE based channel estimator is limited in performance for low and moderate vehicular speeds. Here the work is extended for QR-LS based joint coarse-fine channel estimator [49]. As mentioned earlier, the proposed QR-RLS based MIMO time domain channel estimator better tracks the coarse component of the channel in time domain. Once the coarse component is estimated, fine component of the channel is found out in frequency domain using scattered pilots as shown in Fig. (4.1). This leads to better channel tracking compared to only pilot based linear estimation in fast fading channels.

4.2.2 Pilot Based Fine Estimation

As mentioned previously, PRU is the smallest resource allocation unit in a subframe, which contains data as well as pilot subcarriers. Let the number of data burst transmitted in a subframe be Nd. Within a subframe, Nd data burst is allocated in Np PRUs. Therefore, pilots per subframe per stream are Nd·Np. For simplicity Nt = Nr = 4 is considered, and number of data stream is also 4. Pilots per PRU per data stream is 4 as shown in Figs. (4.1) and (3.5) [23]. Since the frame preamble symbol is referenced at time n, then OFDM symbols will occur at time $n+1, n+2, n+3$.... Let the $Xp_{qk}(n+1)$ and $Yp_{qk}(n+1)$ denote the transmitted and received pilot subcarriers at time $n+1$ at q^{th} antenna and k^{th} subcarrier. Then the channel at time $n+1$ is given by

$$\hat{H}p_{qk}(n+1) = Yp_{qk}(n+1)/Xp_{qk}(n+1) \tag{4.1}$$

Also Eq. (2.16) provides preamble based time domain channel component $\bar{H}_q$. Taking FFT provides $FFT(\hat{H}q) = \hat{H}pre_q(n)$ where $\hat{H}pre_q(n)$ denotes the estimated channel at the q^{th} antenna at preamble symbol at time n. Now at the initial stage, let $(\hat{H}p_{qk}(n)) = \hat{H}pre_q(n)$ (since the first symbol of frame is preamble symbol). Then by using Eq. (4.1) with $(\hat{H}p_{qk}(n))$, fading parameter Dop_a at time $n+1$ for i^{th} subband is derived as shown in Fig. (4.1) given by

$$Dop_a(n+1,i) = \frac{1}{(N_1)} \cdot \sum_{k=0}^{N_1} \hat{H}p_{qk}(n+1)/\hat{H}p_{qk}(n), \tag{4.2}$$

Using the above Eq. (4.2), where N_1 = 2 or 4 depepnds on channel fast/slow fading. Channel at every subcarrier at time $n+1$ is calculated as follows:

$$\hat{H}p_q(n+1) = Dop_a(n+1) \cdot \hat{H}p_q(n) \tag{4.3}$$

For channel estimation at next OFDM symbol, $(\hat{H}p_{qk}(n+1))$ becomes $(\hat{H}p_{qk}(n))$ and the above three equations Eq. (4.1),(4.2) and (4.3) are repeated with time n. As seen in Fig. (3.5), pilots are not transmitted for every 3^{rd} symbol. In such a case, Dop_a is derived from the next symbol and channel is estimated. Channel coefficients for 3^{rd} symbol is then derived by averaging the two nearest symbols, i.e. 2^{nd} and 4^{th} symbol in this case.

4.2.3 Simulation Results

Simulations are provided here for various pilot interpolation based channel estimators. It provides comparison of various interpolation methods in terms of performance and complexity. This

is used as a refrence to select the best complexity and performance trade off method to be used for comparision with the proposed estimator.

Pilot Interpolation Based Estimation for Flat Fade Channel

Nominal Channel B.W. = 10 MHz
Fs = 11.2 MHz
T = 1/Fs = 89.2 ns
FFT Size = 1024
ΔF = 10.9375 kHz
Pilot Boost = 16/9
Ts $\approx$ (1 / ΔF) = 92e-6
Channel: Flat Fading channel, 3 km/hr, Veh-A, Ped-B
Flat Fading channel PDP:
delays = [0 60 110 170 240 290 340 390] nsec;
powers = [0 -5.2 -4.7 -9.9 -13.7 -18.0 -22.4 -26.7];
Veh-A PDP:
delays = [0 310 710 1090 1730 2510];
powers = [0.0 -1.0 -9.0 -10.0 -15.0 -20.0];
Ped-B PDP:
delays = [0 200 800 1200 2300 3700];
powers = [0.0 -0.9 -4.9 -8.0 -7.8 -23.9];

Tmax = 390e-9 (Flat Fade),2510e-9(Veh-A), 3700e-9(Ped-B)
Modulation : BPSK, 64-QAM
Pilot Spacing : less than DT, DF (Throughout simulation considered 4, reason given below[19])
DT (Spacing in time Direction between two pilots) = 1/(Doppler-spread $\cdot$ Ts)
DF (Spacing in freq. Direction between two pilots) = 1/(Tmax $\cdot$ ΔF)
Doppler-spread : 25.2, 252 (for operating freq. 9.1 GHz, speed 3, 30)
For 25.2, 252, cases , DT $<$ 10 . Tmax = 3700ns, ΔF = 10.9375khz, DF $\leq$ 6.

Here simulation results of various interpolation methods like MMSE [34], linear [7], interp (interp matlab function) and DFT-IDFT [67] are shown for refrence. The MMSE interpolation method used here for comparision is based on preassumption of maximum delay spread and doppler spread as given in [19][34]. Time-Freq. grid with period of coherence time and coherence bandwidh is considered. All the simulation results shown here are only for frequency direction, taking

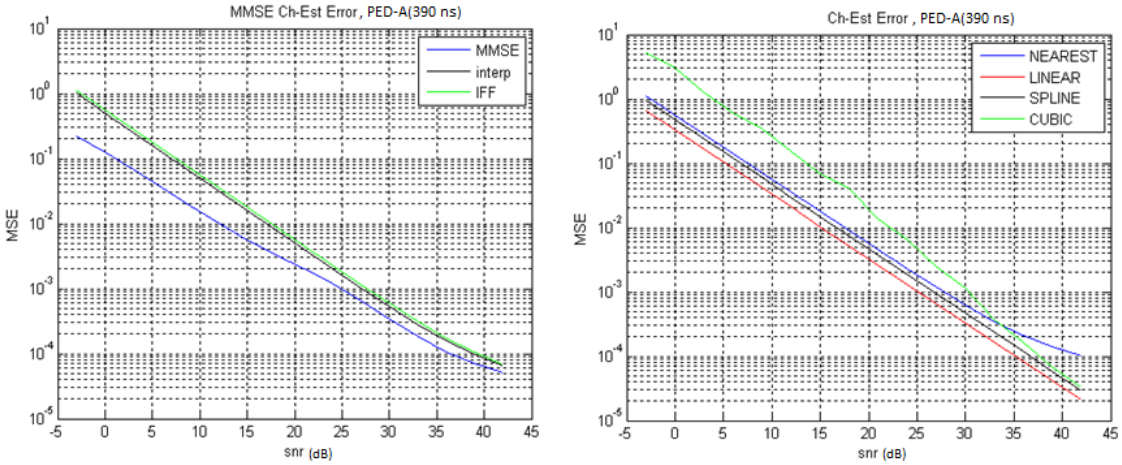

Figure 4.2: Various Pilot Interpolation Methods For Flat fade(PED-A) channel

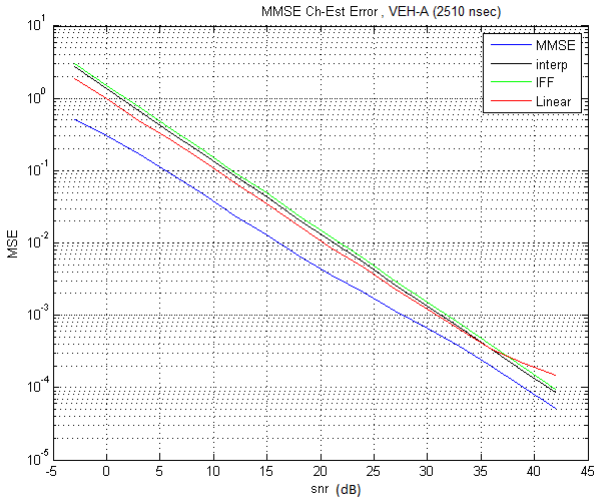

Figure 4.3: Various pilot interpolation for VEh-A

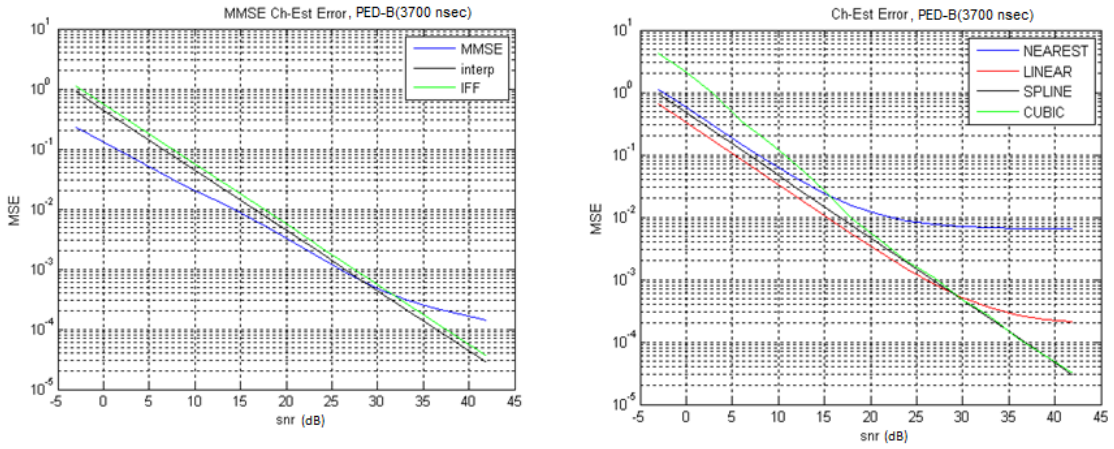

Figure 4.4: Various pilot interpolation for PED-B

care of frequency selectivity of channel. Since pilots are also spaced with spacing of coherence time, results can be extended similarly for time direction to track fast fading channels. The results in Fig. (4.2)-(4.4) show that various pilot interpolations almost give similar performance when pilots are spaced with consideration of delay spread and doppler spread. For channels with small delay spread (i.e. 390 ns Fig. (4.2)) MMSE and linear estimator provide better performance compared to other estimators. However, as delay spread of the channel increases (i.e. Figs. (4.3) and (4.4)), it can be seen from results that second order spline and cubic spline interpolations better fit the curvature of channel frequency response and thus are better for frequency selective channels. The overall result shows that all interpolation methods used give 10^{-3} channel estimation error for $\leq$ 30 dB.

Complexity Compaision of Interpolation Methods

Let's assume, N_{sc} = 1024 is the number of useful subcarriers and N_p= 256 is the number of pilot subcarriers. Then the number of computations for various interpolation methods are given as in Table 4.1.

Nearest Neighbor : zero multiplication and additions.

let N_{sc} subcarriers are divided into Nc clusters. Cluster size = 16, No of clusters = 64,

Then following MMSE estimator given in [7][34], number of complex multiplications and addition per cluster is

For Autocorr Mtx. inv of size 4x4 = 64 (since 4 pilots per cluster, so Autocorr mtx size is 4x4)

For Crosscorr Mtx. of size 4*(16) = 64

Table 4.1: Complexity of All Pilot interpolation Methods for given simulation parameters

Method	Complexity in MAC units
$NearestNeighbor$	0
$Linear$	1024
$CubicSpline$	4×1024
$IFFT/FFT$	$2((256)log_2(256))$
$MMSE$	4480

For finding Complex Weights = 256
To find the estimates = 64
TOTAL = 64+64+256+(64*64) = 4480 complex multiplications and additions

From BER performance and complexity viewpoint, linear interpolation is considered for comparison with the proposed estimator due to its lowest computational complexity among all interpoation methods (except nearest neighbourhood method) while meeting almost near optimum performance as in Fig. (4.2)-(4.4).

Preamble-Pilot based Joint QR-LS Estimation

Frame size : 8 subframe
OFDM symbols per subframe : 5
First Symbol of each frame is SA-Preamble symbol
FFT size : 2048
Fs : 22.4 MHz
fc : 2.5849 Ghz
Channel profile :
Ped-A 5-30 Km/Hr, Veh-A 30-120 Km/Hr
Modulation Type : QPSK,16-QAM

Here also pilot spacing considers Delay spread and Doppler spread.
For ex. suppose maximum vehicular speed is 320 km/hr,
Fdmax = V·Fc/C = 765.896
Coherence time $\approx$ 1/Fdmax = 1/756.896 = 1.3 msec
Ts = 103 μsec
Pilot scattering in time direction can be DT = 1300/103 $\approx$ 12 OFDM symbols without any loss. However here separation is only 5/6 OFDM symbols[23] $\approx$ 515 μsec.

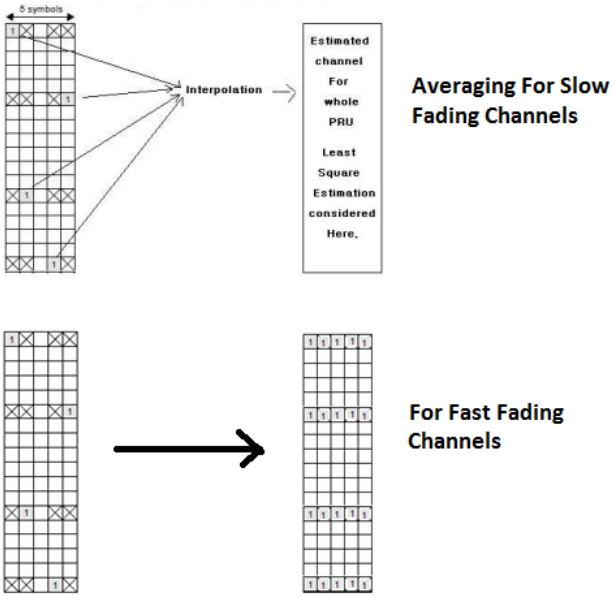

Figure 4.5: Pilot Interpolation for Slow/Fast fading Channels

Similarly, Considering Maximum Delay Spread for PED-B is 3700 nsec.
Tmax = 3700 nsec
Coherence BW $\approx$ 1/(3700e-9) = 270 KHz
Fs = 22.4 Mhz
Carrier-Spacing δF = 22.4e+6/2048 = 10.93 KHz
so pilots can be transmitted 270 khz apart in freq. direction in Time-Freq. grid, However here separation is $\approx$ 180KHz[23]. This fulfills the required criteria.
Simulation results for channel estimation error and BER performances are shown in Fig. (4.6)-(4.8). BER performances for QR-LS coarse-fine estimator is compared with only scattered pilot based linear estimation as in Fig. (4.5). Results in Figs. (4.7) and (4.8) are under similar channel environment, but the pilot interpolation criteria is changed from slow to fast fade as shown in Fig. (4.5).

In Fig. (4.6) BER performance is given for Ped-A channel. Since it is slow fading channel, pilots within the smallest data unit (PRU) of size $Nsc \cdot Nsym$ (here $18 \cdot 5$) are averaged. This value is assigned as channel estimated value for the whole block. The result shows that the proposed estimator gives slightly better performance compared to pilot averaging method. In Figs. (4.7)-(4.8) BER performance is given for Veh-A channel. Veh-A channel being a fast fading channel, pilot

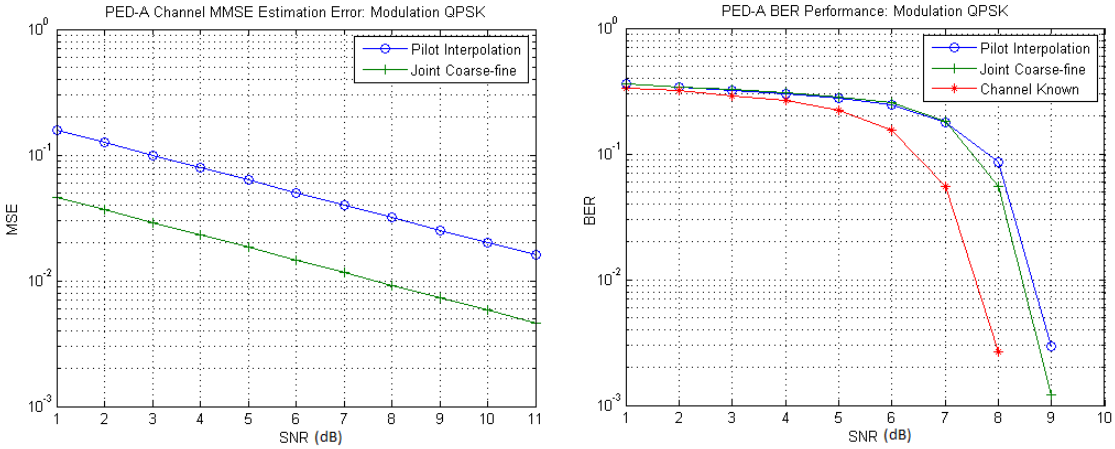

Figure 4.6: PED-A Channel

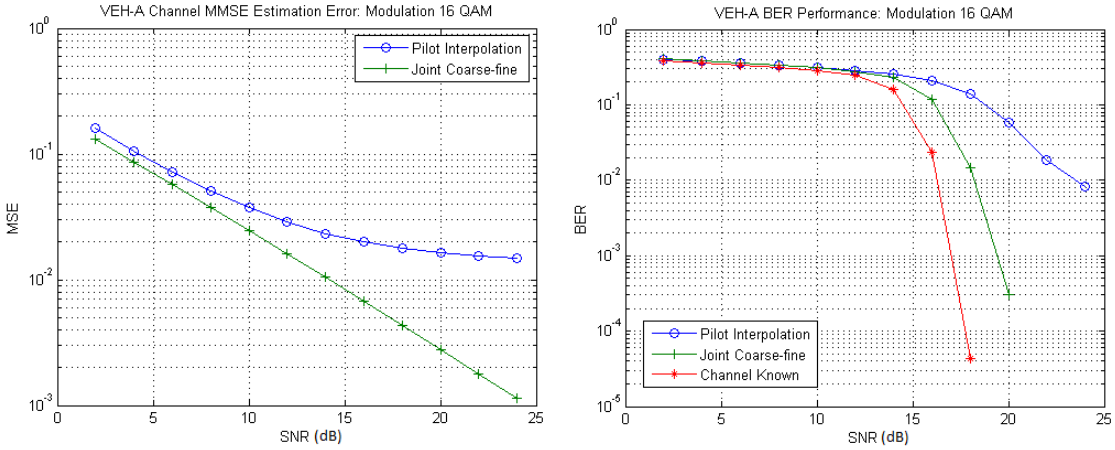

Figure 4.7: VEH-A Channel

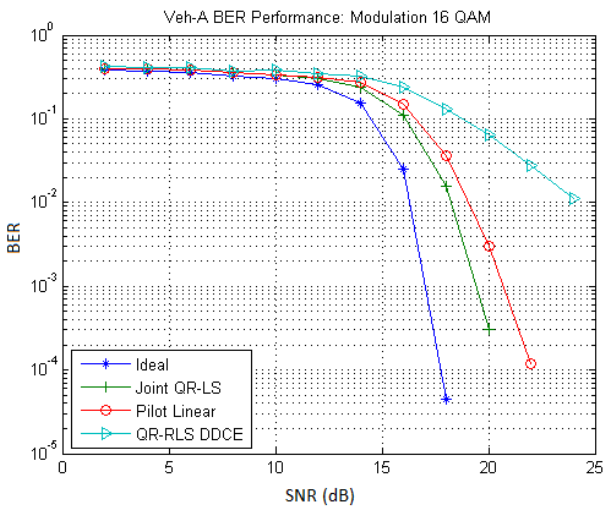

Figure 4.8: VEH-A with Different pilot interpolation configuration

averaging based estimator cannot follow the channel variations effectively, so pilots are interpolated as shown in Fig. (4.5). Results show that the proposed estimator leads to better result than both pilot interpolation configuration in slow as well as fast fading channel conditions. Fig. (4.8) shows the performance comparison with QR-RLS DDCE method for reference. It clearly shows that the proposed method better tracks the fast variations of channel compared to QR-RLS DDCE method. However, this additional gain of proposed method over pilot interpolation method/QR-RLS DDCE method comes with some additional complexity. This additional complexity can be directly seen by comparing Table 2.1 with Table 4.1.

Chapter 5

SM-MIMO Detection and EVS Problem

5.1 Coherent Detection Requirement II : SM-MIMO DATA Detection

5.1.1 Background and Previous Methods

The next generation communication systems demand for transmission speed from 100Mbps (in vehicular) to 1Gbps (in pedestrian) to meet the future communication needs. Since many investigations in the past few years have shown that multiple antenna systems provide an enormous increase in capacity compared to Single Input Single Output (SISO) systems [59], a Multiple Input Multiple Output (MIMO) system is considered as one of the possible techniques. A MIMO technique is classified into two categories: Spatial Diversity (SD) and Spatial Multiplexing (SM). Using MIMO systems [60],[17] enables us to achieve high data rates or reduce the effective error rate on a rich scattering wireless channel. In general, SD technique is simple at the receiver. However, it significantly reduces capacity [53],[12]. In order to meet the requirement of the high data rate, SM method which transmits the independent data streams at each transmit antennas is more appropriate than the SD technique.

In this thesis, the work focus on the SM MIMO systems. In SM MIMO system, since independent data streams are transmitted at each transmit antennas without increasing transmit power and spectral bandwidth, it is considered as one of the possible ways to achieve the high data rate. However, spatial de-multiplexing at the receiver is a challenging task. There are many detection methods which have been actively developed. Among these, exhaustive full search of ML method is considered as the optimum detection method [10]. However, its computational complexity increases exponentially with the number of transmitted antenna and constellation points. The linear

detection methods such as Zero Forcing (ZF) and Minimum Mean Square Error (MMSE) methods have low complexity. However, they undergo a severe performance degradation due to noise enhancement. The OSIC [11],[43] which is known as V-BLAST offers a good trade-off between performance and complexity. Many OSIC-series detectors attempted to reach ML performance with feasible complexity. The OSIC-series detectors such as detectors in [30],[15],[24],[54] are good examples.

The performance improvement in the conventional OSIC is limited due to error propagation, so a successful detection of the first layer is crucial. In an effort to reduce the error propagation, a number of spatial streams are jointly detected in the ML-DFE detection method [5] and then the remaining streams are decoded as in OSIC method. This method mitigates the error propagation. However, the computational complexity due to joint detection is quite high and performance improvement is quite limited. In [25], by assigning all the constellation points to the Most Reliable Layer (MRL), a performance improvement was observed over the conventional OSIC. A sub-optimum QRM-MLD detection method is proposed in [30],[15], where the channel matrix is decomposed into a unitary matrix Q and an upper triangular matrix R, and the M-best nodes are selected at each layer or spatial stream. At the last stage, the ML metrics for the M candidate vectors are compared to decide the best estimate of the transmitted vector.

In [54], the authors asserted that the selection of the Least Reliable Layer (LRL) is a more effective way to mitigate the error propagation, when all the constellation points are assigned to the first layer symbol. The hard-output performance of QR-LRL approaches the ML performance with simple hardware complexity. They also provided soft-output solution for channel decoder [16][54]. However, their solution for soft-output generation is not good enough to deal with empty vector set problem, especially if the modulation order is low. Since as the modulation order increases, the probability of a candidate vector set having all constellation point at each layer increases, which in turn lessen/soothe EVS[26]. Several remedies [16][65][54] are used to find out soft values in the presence of empty vector set, but are not very performance effective. In [26] the author provided a solution to remove empty vector set problem by taking multiple QR decomposition of ordered channel matrix and trying every constellation point at each layer. However, such a solution comes with increased complexity. In [28] the author provided a solution to mitigate empty vector set problem by assigning every constellation point at each layer, where he uses QR matrix transformation while avoiding computation of multiple QR decomposition.

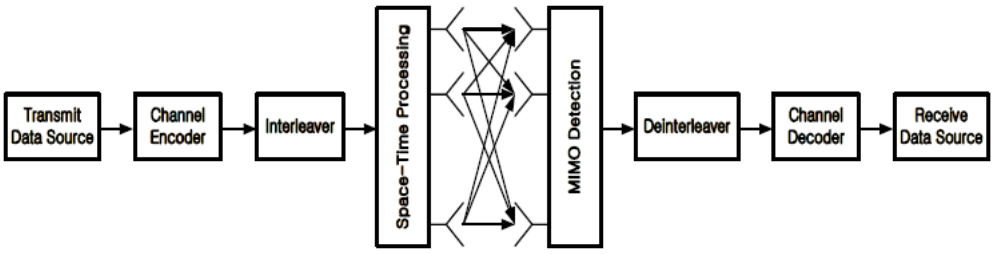

Figure 5.1: MIMO MODEL

5.1.2 MIMO System

In this section, the MIMO system is described. After that various SM-MIMO detectors, EVS problem and it's remedies are described.

MIMO System Description

A MIMO system with m transmit antennas and n receive antennas is considered. The conventional MIMO system is showed in Fig.(5.1), and received signal y can be expressed as follows:

$$\mathbf{y} = \mathbf{H}\mathbf{x} + \mathbf{z} \tag{5.1}$$

$$\begin{pmatrix} y_1 \\ y_2 \\ . \\ . \\ y_m \end{pmatrix} = \begin{pmatrix} h_{1,1} & h_{1,2} & . & . & h_{1,m} \\ h_{2,1} & h_{2,2} & . & . & h_{2,m} \\ . & . & . & . & . \\ . & . & . & . & . \\ h_{n,1} & h_{n,2} & . & . & h_{n,m} \end{pmatrix} \begin{pmatrix} x_1 \\ x_2 \\ . \\ . \\ x_m \end{pmatrix} + \begin{pmatrix} z_1 \\ z_2 \\ . \\ . \\ z_m \end{pmatrix}$$

where, x_i, $i = 1, 2, ...m$ is the transmitted signal from the i^{th} transmit antenna,
y_j , $j = 1, 2, ...n$ is the received signal at the j^{th} receive antenna,
$z_j <= CN(0, \sigma^2)$, j = 1, 2,...n is the circularly symmetric white Gaussian noise,
h_{ji}, $j = 1, 2, ...n, i = 1, 2, ...m$ is the uncorrelated channel coefficient between the j^{th} receive antenna and the i^{th} transmit antenna. In this thesis, transmitted symbols are the QAM modulated symbols.

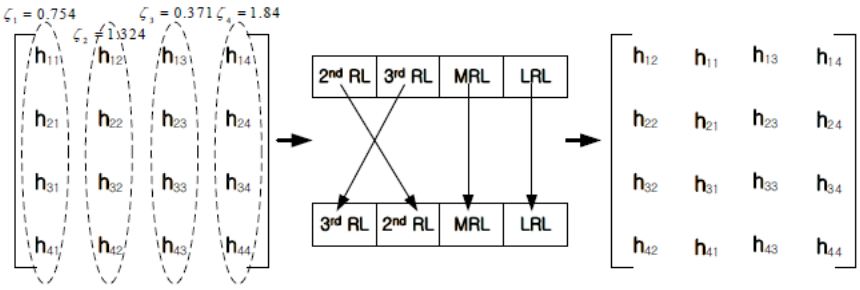

Figure 5.2: QRLRL-ORDER

5.2 QR-LRL Based SM-MIMO Detector

Hard-Output QR-LRL Method [54]

In an effort to exactly detect the first layer symbol compared to conventional QR-OSIC [Appendix 2], the author suggested QRMRL [25]. In QR-MRL, all constellation points are assigned to the first layer symbol instead of deciding it. Also, the channel matrix is ordered by selecting MRL as the first detection layer. However, when all the constellation points are considered for first layer symbol, selection of the MRL in ordering is not an effective way to mitigate the error propagation. In QR-LRL [54], by assigning the LRL to the first layer, the error propagation is more reduced than the QR-MRL. Moreover, QR-LRL detection method can achieve near ML performance. The ordering to find the LRL is important in QR-LRL, so that the post-detection SNR ζ is used for the layer ordering. The detailed ordering process in QR-LRL is summarized in Fig. (5.2).

$$\mathbf{y} = \mathbf{H}_{ordered} \cdot \mathbf{x}_{ordered} + z \tag{5.2}$$

$$\mathbf{H}_{ordered} = [h^{(m-1)^{th}RL}; .....h^{3ndRL}; h^{2ndRL}; h^{MRL}; h^{LRL}]$$

$$\mathbf{x}_{ordered} = [x^{(m-1)^{th}RL}; .....x^{3rdRL}; x^{2ndRL}; x^{MRL}; x^{LRL}]$$

After obtaining the system equation and applying every constellation point at each layer, the Euclidean metric is calculated and minimum distance vector is chosen as the optimum detected vector to achieve hard ML performance. The detection process in QR-LRL is equal to QR-MRL [Appendix 2][25] except detection layer ordering. The LRL is chosen based on post detection SNR, which is $\parallel g_i \parallel^2$, $i = 1.2.3...m$ as in [54], where $G = ((H^T H)^{(-1)} H^T)$. The whole method is described in Table (5.1).

Table 5.1: Psuedo code for QR-LRL .

$QRLRL - SMMIMO - Detector$
$\mathbf{function}[V] = QR - LRL(\mathbf{y}, \mathbf{H}_{ordered})$
$[Q, R] = qr(H_{ordered})$
$for \;\; i = 1 : \|C\|$
$x_{(4)} = C(i)$
$x_{(3)} = Q(\frac{\bar{y}_3 - r_{34}x_{(4)}}{r_{33}})$
$x_{(2)} = Q(\frac{\bar{y}_2 - r_{23}x_{(3)} - r_{24}x_{(4)}}{r_{22}})$
$x_{(1)} = Q(\frac{\bar{y}_1 - r_{12}x_{(2)} - r_{13}x_{(3)} - r_{14}x_{(4)}}{r_{11}})$
$V(:, i) = [x_{(1)}, x_{(2)}, x_{(3)}, x_{(4)}]^T$
$Dist(:, i) = \|\|\mathbf{y} - \mathbf{H}_{ordered} \cdot (V(:, i))\|\|.^2$
end

5.3 Empty Vector Set Problem and Previous Remedies

5.3.1 Soft-output Generation

It is well known that Bit-Interleaved Coded Modulation (BICM) can achieve the open loop capacity when proper soft-output values can be provided to the channel decoder at the receiver. Consequently, the capability of soft-output generation is very important for good overall system performance. BICM allows a different Maximum A Posteriori (MAP) based decoding scheme in which the received QAM signals are first demodulated by a soft-output demapper and de-interleaved, and then passed to a standard binary soft-input soft-output viterbi or turbo decoder. The idea is to demap the received signal into soft bits, which has the same sign as provided by a hard detector and whose absolute value indicates the reliability of the decision.

5.3.2 Empty Vector Set

In SM MIMO systems, Log Likelihood Ratio (LLR) or soft output values generally achieve open loop capacity. Generally LLR for the k^{th} bit in i^{th} symbol of received vector y is given by

$$L(b_{k,l}|\mathbf{y}) = ln\frac{Pr[b_{i,k} = 1|\mathbf{y}]}{Pr[b_{i,k} = 0|\mathbf{y}]} \tag{5.3}$$

Where $Pr[b_{i,k} = 1|\mathbf{y}]$ is the probability for k^{th} (k ranging $0 \rightarrow log_2|C|$) bit in i^{th} (i ranging $1 \rightarrow N_T$) symbol. Since it is very cumbersome to calculate Eq. (5.3), the LLR value for the k^{th} bit

in l^{th} symbol, $k = 1, 2...log_2|(C)|$, $l = 1, 2, ...m$ can be approximated as

$$L(b_{k,l}|\mathbf{y}) \approx \min_{\mathbf{x} \in S(k,l)^- \subset V} D(\mathbf{x}) - \min_{\mathbf{x} \in S(k,l)^+ \subset V} D(\mathbf{x}) \tag{5.4}$$

Where $S(k,l)^-$ is the candidate vector set corresponding to $b_{k,l} = -1$, $S(k,l)^+$ is the candidate vector set corresponding to $b_{k,l} = +1$, C denotes constellation point set and $|C|$ is it's size. The distance metric is given by

$$D(\mathbf{x}) = \frac{1}{\sigma^2} \cdot \| \mathbf{y} - \mathbf{Hx} \|^2$$

V is the candidate vector set obtained after all layer symbol detection. It is possible that either $S(k,l)^-$ or $S(k,l)^+$ is an empty set as shown in Fig. (5.3), which causes hindrance in generating LLR.

5.3.3 Previous Remedies

Threshold in QRM-MLD Detector [16]

QRM-MLD [30][Appendix2] signal detection method performs the generation of LLRs in the last stage, so it always suffers from the empty vector set problem. Therefore, in [16], the authors proposed the likelihood function generation method for non-existing bit, which can mitigate the empty vector set problem. In the proposed scheme, LLR generation method is described in the following process:

- The symbol replica candidates among the remaining symbol replica candidates in the last stage, which bit '1' or '-1' remains, are selected independently.
- For the symbol replica candidates selected for each bit '1' and '-1', the likelihood function of each bit for each symbol replica is obtained using the Euclidean distance for selected symbol replicas.
- For each bit in the data symbols, the likelihood function of bit '1' is derived as the minimum Euclidean distance among candidates of the Euclidean distance obtained in the second step. The likelihood function for bit '-1' is obtained in the same manner.
- For a bit, which has both bits '1' and '-1' in the remaining symbol replica candidates in the last stage (let NB be the number of bits which has both bits '1' and '-1' in the remaining symbol replica candidates in the last stage), the larger likelihood function of two bits, '1' or '-1', is selected.

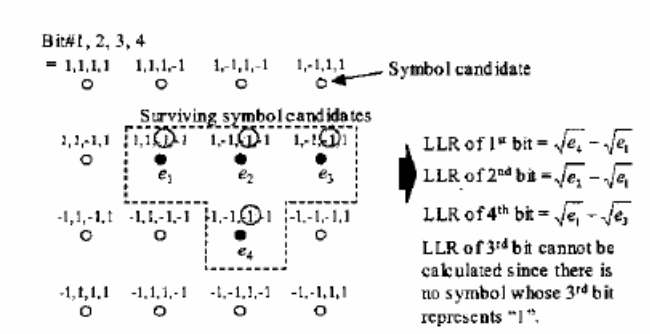

Figure 5.3: Empty-Vector-Set-Problem

- Among the bits, which have both bits '1' and '-1' in the remaining symbol replica candidates in the last stage, the selected larger likelihood function of each bit in the data symbols are summed (note there are NB bits) and its summation is normalized by NB.
- Finally, the likelihood function calculated in the previous step is multiplied by a factor of 'X'. This value is used for the symbol candidates suffering from Empty Vector Set problem. Author [16] uses value of $'X = 1.5'$ based on simulation environment.

Threshold in QR-LRL Detector [54]

Since each constellation point is tried at LRL, $S(k,l)^-$ and $S(k,l)^+$ will not be an empty set at LRL. Using this property threshold value Th is derived at LRL[54], which is used for calculating LLR for the bits suffering from EVS at higher layers. At first, LLR at LRL corresponding to $x(m)$ (where m varies from $1, 2...|C|$) is calculated as

$$L_D(b_{k,(m)}|\mathbf{y}) \approx \min_{\mathbf{x}\in S(k,(m))^-} D(\mathbf{x}) - \min_{\mathbf{x}\in S(k,(m))^+} D(\mathbf{x}) \tag{5.5}$$

$$T^+(k) = \min_{\mathbf{x}\in S^+_{(k,(m))}} D(\mathbf{x}), 1<k \leq log_2|C| \tag{5.6}$$

$$T^-(k) = \min_{\mathbf{x}\in S^+_{(k,(m))}} D(\mathbf{x}), 1<k \leq log_2|C| \tag{5.7}$$

$$T(k) = max(T^+(k), T^-(k)), 1<k \leq log2|C| \tag{5.8}$$

From above Eq. Threshold value $'Th'$ is derived as

$$Th = \frac{1}{log_2|C|} \sum_{k=1}^{log_2|C|} T(k) \tag{5.9}$$

This threshold is used for calculating LLR for the bits suffering from EVS at higher layers.

Enlarged QR-DD Detector [26]

In QR-DD method, every constellation point is tried at each layer and LLR is calculated using enlarged candidate vector set. For example, consider a 4×4 MIMO system.

- At first, H is ordered according to the minimum error prpagation ordering suggested in [9] with LRL as first detection layer. At the same time, since all constellation points are tried at each layer, the ordering criteria is used with loose ordering method based on SNR instead of post detection SNR [26]. Thus H is ordered $\| \mathbf{h}_i \|^2$, $i = 1, 2, 3, 4$ as shown below.

  $$H_{ordered,1} = [\mathbf{h}_{3rdRL}, \mathbf{h}_{2ndRL}, \mathbf{h}_{MRL}, \mathbf{h}_{LRL}]$$

  Where $\| \mathbf{h}_{MRL} \|^2 > \| \mathbf{h}_{2ndRL} \|^2 > \| \mathbf{h}_{3rdRL} \|^2 > \| \mathbf{h}_{LRL} \|^2$. Where $\mathbf{h}_{2ndRL}$, $\mathbf{h}_{3rdRL}$ represents the 2^{nd} and 3^{rd} reliable layer of $\mathbf{h}$ respectively.

- Now using upper QR structure, candidate vector set $V_{S,12}$ is generated for LRL and MRL as per Table 1.
  $V_{S,12} = [V_{cand,1}, V_{cand,2}]$, Where $V_{S,12}$ represents enlarged candidate vector set consist of vectors $V_{cand,1}$ and $V_{cand,2}$. Here $V_{cand,1}$ and $V_{cand,2}$ are vector set corresponding to vectors generated while trying each constellation point at LRL and MRL respectively.

- Again, to apply each constellation point at the remaining two layers i.e. 2^{nd} and 3^{rd} detection layer, H is reordered as shown below.

  $$H_{ordered,2} = [\mathbf{h}_{LRL}, \mathbf{h}_{MRL}, \mathbf{h}_{3rdRL}, \mathbf{h}_{2ndRL}]$$

  Applying QR decomposition on reordered H, $V_{S,12}$ is generated for the remaining two layers, 2^{nd} and 3^{rd} reliable layer using Table (5.2), where $V_{S,12} = [V_{3rdRL}, V_{2ndRL}]$. Here $V_{S,12}$ represents enlarged candidate vector set which consists of vectors V_{2ndRL} and V_{3rdRL}, where V_{2ndRL} and V_{3rdRL} are vector sets corresponding to vectors generated while trying each

Table 5.2: Candidate Vector Set at LRL,MRL layer .

$function[V_{S,12}] = CandidateV_{12}(\mathbf{y}, \mathbf{H}_{ordered})$
$[Q, R] = qr(\mathbf{H}_{ordered})$
$for\ i = 1 : |C|$
$x_{(4)} = C(i)$
$x_{(3)} = Q(\frac{\bar{y}_3 - r_{34}x_{(4)}}{r_{33}})$
$x_{(2)} = Q(\frac{\bar{y}_2 - r_{23}x_{(3)} - r_{24}x_{(4)}}{r_{22}})$
$x_{(1)} = Q(\frac{\bar{y}_1 - r_{12}x_{(2)} - r_{13}x_{(3)} - r_{14}x_{(4)}}{r_{11}})$
$V_{cand,1}(:, i) = [x_{(1)}, x_{(2)}, x_{(3)}, x_{(4)}]^T$
$Dist_{cand,1}(:, i) = ||\mathbf{y} - \mathbf{H}_{ordered} \cdot (V_{cand,1}(:, i))||.^2$
end
$for\ i = 1 : |C|$
$x_{(3)} = C(i)$
$x_{(4)} = Q(\frac{\bar{y}_3 - r_{33}x_{(3)}}{r_{34}})$
$x_{(2)} = Q(\frac{\bar{y}_2 - r_{23}x_{(3)} - r_{24}x_{(4)}}{r_{22}})$
$x_{(1)} = Q(\frac{\bar{y}_1 - r_{12}x_{(2)} - r_{13}x_{(3)} - r_{14}x_{(4)}}{r_{11}})$
$V_{cand,2}(:, j) = [x_{(1)}, x_{(2)}, x_{(3)}, x_{(4)}]^T$
$Dist_{cand,2}(:, i) = ||\mathbf{y} - \mathbf{H}_{ordered} \cdot (V_{cand,2}(:, i))||.^2$
end
$V_{S,12} = [V_{cand,1}, V_{cand,2}]$
$Dist_{S,12} = [Dist_{cand,1}, Dist_{cand,2}]$
$endfunction$

constellation point at $i^{th}RL$ respectively.
Overall, $V = [V_{LRL}, V_{MRL}, V_{3rdRL}, V_{2ndRL}]$

Now V consists of vectors when every constellation point is applied at each layer. EVS problem is effectively removed by this method at the cost of multiple QR decomposition $\approx \lceil \frac{N}{2} \rceil$ for enlarging V. Complexity increases exponentially as $N = min(Nt, Nr)$ increases, where Nt, Nr are number of transmit and receive antennas respectively.

Chapter 6

Proposed Detection Methods to Mitigate EVS

6.1 Proposed Effectively Enlarged Candidate Vector Set of QR-LRL MIMO Detector

The proposed method[46] is an alternative solution to avoid multiple QR decomposition as in [26] and better performance compared to previous remedies [54][16] for soft output generation while mitigating EVS. QR-LRL detector is fully described in [54][26]. From [54], the ordered matrix **H** is used here for deriving candidate vector set.

$$\mathbf{y} = \mathbf{H}_{ordered} \cdot \mathbf{x}_{ordered} + \mathbf{z} \tag{6.1}$$

$$\mathbf{H}_{ordered} = [\mathbf{h}_{(m-1)^{th}RL}, ...\mathbf{h}_{3ndRL}, \mathbf{h}_{2ndRL}, \mathbf{h}_{MRL}, \mathbf{h}_{LRL}]$$

$$\mathbf{x}_{ordered} = [x_{(m-1)^{th}RL}, ...x_{3rdRL}, x_{2ndRL}, x_{MRL}, x_{LRL}]^T$$

Since all constellation points are tried at each layer, the strict layer ordering like post detection SNR is not required. Thus ordering criteria is used with loose ordering method based on SNR, $\| \mathbf{h}_i \|^2$, $i = 1, 2, 3...m$ as in [26].

The proposed algorithm is fully described in Table (6.1) & (6.2). Here, the detection process enlarges candidate vector set at 4 detection layers (LRL, MRL, 2ndRL, 3rdRL) consecutively. For simplicity, an example of the proposed method with 4×4 MIMO system with QPSK modulation (since the number of constellation points is 4) is shown in Fig. (6.1).

STEP 1 : Fig. (6.1) shows that upper triangular structure of R matrix allows to try each con-

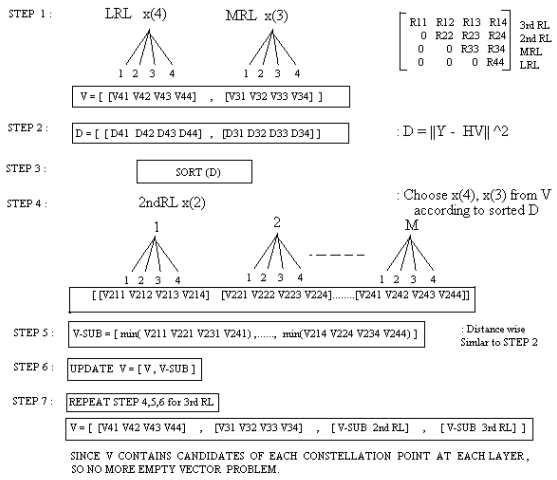

Figure 6.1: Enlarged Candidate Vector set

stellation point effectively at LRL and MRL (first two detected layers) without any other symbol pre-guessing. Enlarged candidate vector set at 1^{st} and 2^{nd} detected layer is given by $V_{cand,1}$ and $V_{cand,2}$ respectively. This ensures that LRL and MRL will no longer suffer from EVS.

STEP 2 : By combining the resultant vectors, candidate vector set at 1^{st} and 2^{nd} detected layer $V_{S,12} = (V_{cand,1}, V_{cand,2})$ is formed i.e.$([V41, .., V44], [V31, .., V34])$ where Vij is candidate vector generated with i^{th} symbol and j^{th} constellation point.

STEP 3 : To effectively prevent error propagation, here least M distance values are chosen according to the sorted distances from the combined set $V_{S,12}$ according to $Dist_{S,12}$, where $M \leq |C|$.

STEP 4 : These M values determine the 1^{st} and 2^{nd} detected symbol when every constellation point is tried at 3^{rd} layer. The resultant vector is $([V211..V214]..[V241..V244])$ where $Vikj$ represnts vector generated by i^{th} symbol k^{th} value from least M values and j^{th} constellation point. Detection at $2ndRL$ follows Table (6.2), where $V_{sM,12}$ is sorted candidate vector set $V_{S,12}$ with least M values.

STEP 5 : Now the candidate vector set ($V - SUB = V_{cand,3}$) is formed using the minimum of groupwise distances for same constellation point at 3^{rd} detection layer i.e. from $min(V(:,k,:))$. Here $(V(:,k,:)) = ([V211..V241]..[V214..V244])$ for $k = 1, 2..M$. For example, If 1^{st} constellation point is applied at 3^{rd} detection layer with LRL and MRL chosen from least M values of $V_{sM,12}$, then $V(:,1,:)$ represents a vector set from which minimum distance vector according to $Dist_3(:,1,:)$ is chosen as a vector with 1^{st} constellation point at 3^{rd} detection layer. Rest of the candidate vectors for 3^{rd} detection layer are found in a similar fashion.

STEP 6 : Once all candidate vectors corresponding to all constellation points at 3^{rd} detection layer given by $V_{cand,3}$ are found, candidate vector set at 3^{rd} detection layer is enlarged by combining

Table 6.1: Candidate Vector Set at LRL,MRL layer .

$function[V_{S,12}] = CandidateV_{12}(\mathbf{y}, \mathbf{H}_{ordered})$
$[Q, R] = qr(\mathbf{H}_{ordered})$
$for\ i = 1 : |C|$
$x_{(4)} = C(i)$
$x_{(3)} = Q(\frac{\bar{y}_3 - r_{34}x_{(4)}}{r_{33}})$
$x_{(2)} = Q(\frac{\bar{y}_2 - r_{23}x_{(3)} - r_{24}x_{(4)}}{r_{22}})$
$x_{(1)} = Q(\frac{\bar{y}_1 - r_{12}x_{(2)} - r_{13}x_{(3)} - r_{14}x_{(4)}}{r_{11}})$
$V_{cand,1}(:, i) = [x_{(1)}, x_{(2)}, x_{(3)}, x_{(4)}]^T$
$Dist_{cand,1}(:, i) = ||\mathbf{y} - \mathbf{H}_{ordered} \cdot (V_{cand,1}(:, i))||.^2$
end
$for\ i = 1 : |C|$
$x_{(3)} = C(i)$
$x_{(4)} = Q(\frac{\bar{y}_3 - r_{33}x_{(3)}}{r_{34}})$
$x_{(2)} = Q(\frac{\bar{y}_2 - r_{23}x_{(3)} - r_{24}x_{(4)}}{r_{22}})$
$x_{(1)} = Q(\frac{\bar{y}_1 - r_{12}x_{(2)} - r_{13}x_{(3)} - r_{14}x_{(4)}}{r_{11}})$
$V_{cand,2}(:, j) = [x_{(1)}, x_{(2)}, x_{(3)}, x_{(4)}]^T$
$Dist_{cand,2}(:, i) = ||\mathbf{y} - \mathbf{H}_{ordered} \cdot (V_{cand,2}(:, i))||.^2$
end
$V_{S,12} = [V_{cand,1}, V_{cand,2}]$
$Dist_{S,12} = [Dist_{cand,1}, Dist_{cand,2}]$
$endfunction$

candidate vector set at LRL and MRL $V_{S,12}$ with $V_{cand,3}$. This results in enlarged candidate vector set $V_{S,13}$.

Again least M (most probably $M = 1$, due to QR-LRL property, higher layers are reliable layers in ascending order) values are chosen from sorted candidate vector set according to distances found similar to STEP 2. These least M values determine previously detected three symbols at respective three layers, while every constellation point is tried at 4^{th} layer i.e. $3rdRL$ and candidate vector set results in $V_{cand,4}$ as in STEP 5. This process goes on until the last layer is detected. Following STEP 6 again, the overall enlarged candidate vector set $V = (V_{LRL}, V_{MRL}, V_{cand,3}, V_{cand,4})$ contains vectors with every constellation point tried at each layer. Thus EVS no longer persists.

Table 6.2: Effectively Enlarge V at 3^{rd} Detection layer .

$function[V_{S,13}] = EnlargeV(\mathbf{y}, \mathbf{H}_{ordered}, V_{S,12}, Dist_{S,12})$
$V_{S,12} = sort(V_{S,12})$
$From- > Dist_{S,12}$
$V_{sM,12} = V_{S,12}(1, 2, ...M) M \leq |C|$
$for\ k = 1 : M$
$x_{(4)} = V_{sM,12}(k, 4)$
$x_{(3)} = V_{sM,12}(k, 3)$
$for\ l = 1 : |C|$
$x_{(2)} = C(l)$
$x_{(1)} = Q(\frac{\bar{y}_1 - r_{12}x_{(2)} - r_{13}x_{(3)} - r_{14}x_{(4)}}{r_{11}})$
$V_3(:, l, k) = [x_{(1)}, x_{(2)}, x_{(3)}, x_{(4)}]^T$
$Dist_3(:, l, k) = ||\mathbf{y} - \mathbf{H}_{ordered} \cdot (V_3(:, , l, k))||.^2$
end
end
$V_{cand,3}(1 : C) = (min(V_3(:, 1, :))..., min(V_3(:, C, :)))$
$From- > Dist_3$
$V_{S,13} = [V_{S,12}, V_{cand,3}]$
$endfunction$

6.1.1 Simulation Results

Simulation results are shown for the proposed method with following specifications. The number of transmit and receive antennas is 4. Rayleigh fading channel is considered. Ideal channel coefficient is assumed to be known at receiver. 1/3 rate Convolutional Turbo Code (CTC) is used as a channel coder, so CTC decoder with 4-5 iteration is used to decode MIMO detected soft information.

Fig.(6.2) shows the performance results for QPSK modulation. In the graph, various combinations of M least distance values for different layers are considered. Value of M_3 represents the number of least values considered for 3^{rd} layer detection from the first two detected layers set, while M_4 considers the number of least values considered for 4^{th} layer detection from previously detected layers set. Figs. (6.3) & (6.4) show the performance result for 16-QAM and 64-QAM respectively. The result shows that large value of M doesn't contribute much in performance (differ by $\leq$ 0.5 dB for various modulation order) while complexity increases sharply. So $M_3 = 2$, $M_4 = 1$ for QPSK and $M_3 = 1$, $M_4 = 1$ for 16QAM, 64QAM are sufficient to achieve near soft ML performance with the lowest complexity. It also shows that as modulation order increases,

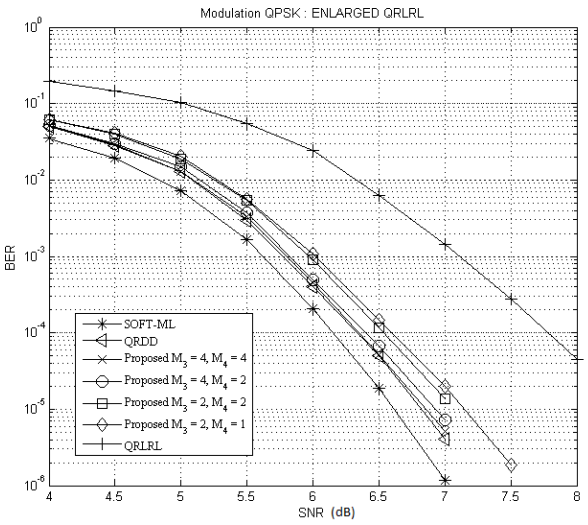

Figure 6.2: Enlarged Candidate set based Soft Output for QPSK

the severity of EVS problem decreases. Figs. (6.4),(6.5) & (6.6) compare performance results of proposed detector ($M_3 = 1$, $M_4 = 1$) 64QAM and ($M_3 = 2$, $M_4 = 1$) for QPSK, 16QAM case with various QR-OSIC detectors. It shows that the proposed method achieves significant gain over conventional methods while matching performance of QR-DD method.

6.1.2 Computation Complexity

Computation complexity of the proposed method for 4×4 MIMO system is shown in Table (6.3). As seen from Figs. (6.2), (6.3) & (6.4), there is no effective performance improvement for higher values of M_3, M_4. So ($M_3 = 2,\ M_4 = 1$) for QPSK and ($M_3 = 1,\ M_4 = 1$) for 16QAM, 64 QAM is considered for complexity consideration of the proposed method.
Complexity for all previous QR-OSIC methods are shown in Table (6.4). where C, M, D and **M** stand for constellation point, order for QR-M, division and multiplications respectively. From Tables (6.3), (6.4) and (6.5), it is clearly seen that for low modulation order ($< 64QAM$), complexity of the proposed method is comparable to QR-LRL method, while it matches QR-DD method for higher modulation order.

Table 6.3: Complexity of Proposed Enlarged QR-LRL

Operation	Complexity	Iteration
$\parallel h_i \parallel^2_{i=1,2,3,4}$	$8\mathbf{M}$	4
$QR_{Decomposition}$	$256\mathbf{M} + 4D$	1
$Q^H\mathbf{y}$	$48\mathbf{M}$	1
$\parallel \mathbf{y} - \mathbf{H}x \parallel^2$	$8\mathbf{M}$	$\lvert C\rvert \times (5)$

$$Total = (5|C| \times 8)\mathbf{M} + 336\mathbf{M} + 4\mathbf{D}$$

Table 6.4: Complexity of All Methods

Method	Complexity
$QRM - MLD$	$(2\times \mid C \mid \times(3M+1))\mathbf{M} + 336\mathbf{M} + 4D$
$QR - LRL$	$(\mid C \mid \times 8)\mathbf{M} + 533\mathbf{M} + 8D$
$QR - DD$	$(4 \mid C \mid \times 8)\mathbf{M} + 640\mathbf{M} + 8D$
$Proposed$	$((2 + M_3 + M_4) \mid C \mid \times 8)\mathbf{M} + 336\mathbf{M} + 4D$

Table 6.5: Complexity of All Methods for Different QAM Order

Type	QRM-MLD	QR-LRL	QR-DD[26]	Proposed
M-QAM	**M + D**	**M + D**	**M + D**	**M + D**
$QPSK$	$440 + 4$	$565 + 8$	$768 + 8$	$476 + 4$
$16QAM$	$1904 + 4$	$661 + 8$	$1152 + 8$	$848 + 4$
$64QAM$	$25040 + 4$	$1045 + 8$	$2688 + 8$	$2384 + 4$

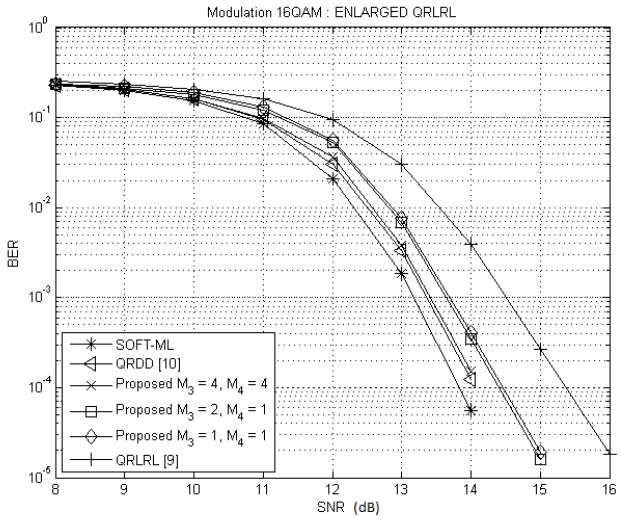

Figure 6.3: Enlarged Candidate set based Soft Output for 16 QAM

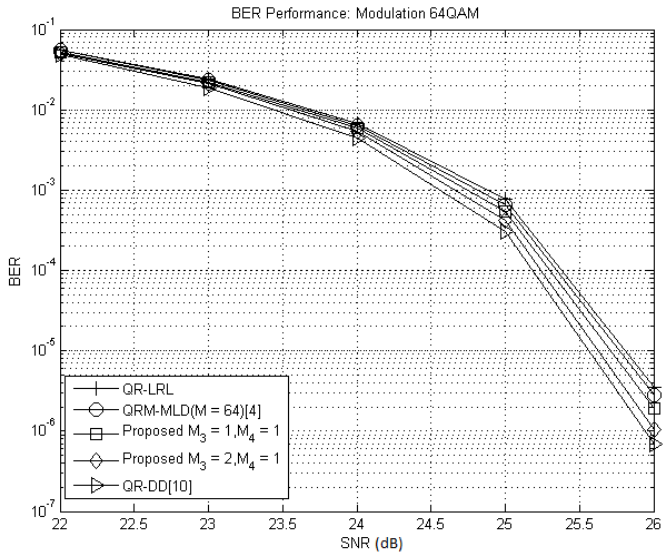

Figure 6.4: BER Performance for Various methods: 64 QAM

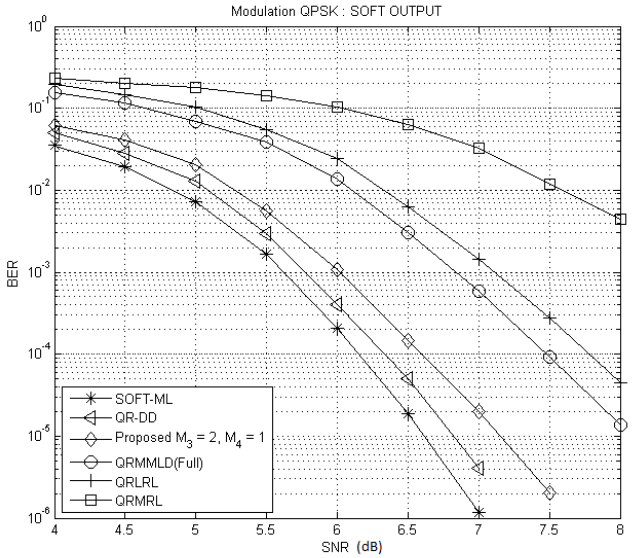

Figure 6.5: Comparision of SOFT BER Performance for various QR-OSIC: QPSK

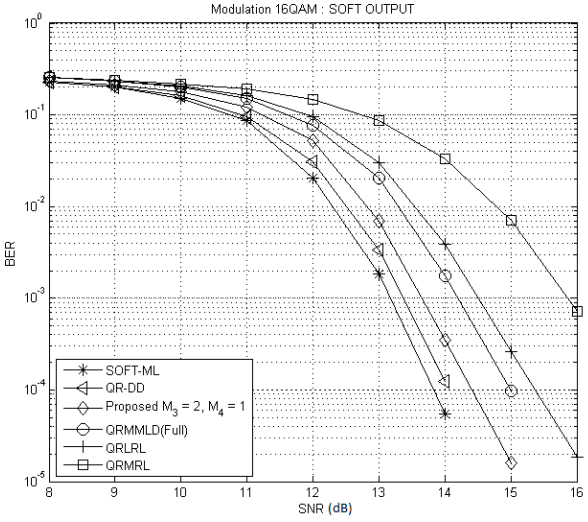

Figure 6.6: Comparision of SOFT BER Performance for various QR-OSIC: 16QAM

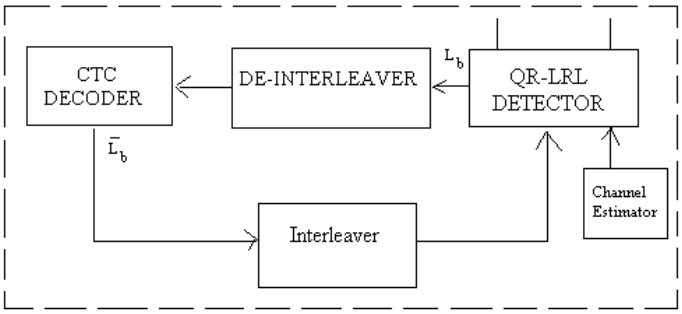

Figure 6.7: Proposed IDD Receiver

6.2 Proposed JIDD Receiver to Lessen/Soothe EVS

Proposed JIDD Receiver[50]:

An Iterative Detection and Decoding(IDD) [33][32][22][69] receiver is shown in Fig. (6.7). It consists of a source encoder, an interleaver and SM-MIMO mapper. Receiver consists of MIMO detector which incorporates channel estimator, de-interleaver and source decoder. Use of interleaver between source decoder and MIMO detector effectively removes error burst due to channel fading.

The proposed decision feedback IDD for mitigating EVS using extrinsic gain of Turbo decoder is described below.

- Candidate vector set V is generated using QR-LRL detector as per Table (5.1).
- Soft LLR values are generated using candidate vector set V and passed to Convolution Turbo Code (CTC) decoder.
- CTC decoder uses 4-5 internal iterations to maximize extrinsic gain which is fed back to MIMO detector.
- For simplicity, initially let LLR values at Turbo decoder input and output for m MIMO layers be

$$L(b_{1:m,l}|y) = [L(b_{1,l}|y), L(b_{2,l}|y), L(b_{3,l}|y).....L(b_{m,l}|y)]$$
$$L(\bar{b}_{1:m,l}|y) = [L(\bar{b}_{1,:}|y), L(\bar{b}_{2,l}|y), L(\bar{b}_{3,l}|y).....L(\bar{b}_{m,l}|y)]$$

where l varies from 1,2...$log_2 C$.

- Using hard decisions on Turbo decoder output $L(\bar{b}_{1:m,l}|y)$, new candidate is formed as

$$V_X(1:m) = [\bar{x}(m), \bar{x}(m-1), \bar{x}(m-2).....\bar{x}(1)]$$

$$D_X = ||\mathbf{y} - \mathbf{H}_{ordered} \cdot (V_X)||.^2 \tag{6.2}$$

- Similarly using $V_{\bar{X}}$ in QR-LRL method as m detected symbols, new vector is formed as

$$\hat{V}_X(1:m) = [.....Q(\frac{y - r_{m-1,m} \cdot V_{X(m)}}{r_{m-1,m-1}}), V_{X(m)}]$$

This vector is already available in original candidate vector set, but here is represented in this form for ease of understanding.

$$\hat{D}_X = ||\mathbf{y} - \mathbf{H}_{ordered} \cdot (\hat{V}_X)||.^2 \tag{6.3}$$

- Error propagation is prevented using metric which is

$$Min_D = min([Dist(:,i), D_X, \hat{D}_X])$$

with two conditions, where $Dist(:,i)$ is from Table (5.1), D_X and $\hat{D}_X$ are from Eq.(6.2) and (6.3) respectively.

- Conditions :
  1. If Min_D is $Dist(:,i)$ set, then previous LLR values are passed without any change to the Turbo decoder.
  2. However, if Min_D is among D_X or $\hat{D}_X$ then corresponding candidate vector in V set which consist of 1,2...‖C‖ candidate vectors is updated.

- Since QR-LRL soft detection method is considered here, updating is done by replacing corresponding candidate vector in candidate vector set V whose first symbol matches with the minimum distance vector. For example, if Min_D corresponds to D_X then candidate vector in V, whose first symbol matches first symbol of V_X is updated and new LLR value is generated.

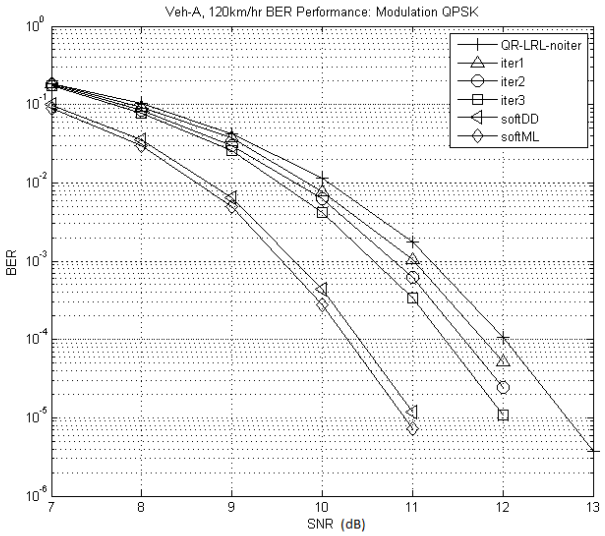

Figure 6.8: BER Performance Of Iterative QR-LRL for QPSK

6.2.1 Simulation Results

Simulation results are shown for the proposed method with following specifications. Monte Carlo simulations are performed for 1000-1500 subframes of 802.16m (Mobile Wimax) standard. The number of Tx., Rx. antennas is 4. QPSK and 16QAM modulation types are considered. Veh-A channel is considered with mobile speed of 120 km/hr. Channel coefficients are derived using COMB pilots and used for QR decomposition of channel matrix. CTC decoder 4-5 internal iteration is used to decode MIMO detected soft information. Extrinsic gain is achieved from internal CTC iterations.

Fig. (6.8) shows the performance results for QPSK modulation. It shows that with increasing number of outer iterations (2-3) significant gain is achieved. Similarly, Fig. (6.9) shows the performance results for 16QAM modulation. The results are compared with $softML$[10], $SoftDD$[26] performances.

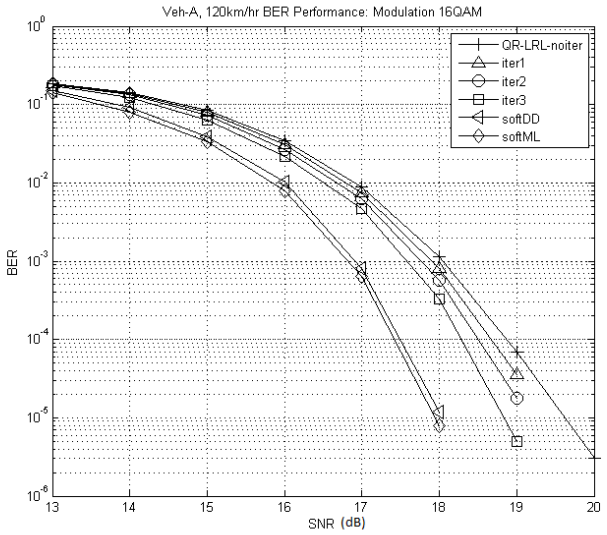

Figure 6.9: BER Performance Of Iterative QR-LRL for 16-QAM

Chapter 7

Conclusion

In the presented work, two problems related to coherent detection for MIMO-OFDM system are addressed. One is channel estimation and the other is EVS mitigation during soft output generation. QR-RLS adaptive method is extended for time domain adaptive MIMO-OFDM cannel estimation. Simulation results show that the proposed estimator gives near optimum perfromance while avoiding matrix inversion as in RLS estimator. It also doesn't require prior statistical information as in MMSE estimator. Results also show that MMSE estimator is the best estimator with the highest complexity while frequency domain least square estimator is the worst with lowest complexity. The proposed estimator comes in between these two estimators in terms of performance as well as complexity. Convergence result of the proposed estimator at different SNR values gurantee for $\leq$ 10 $\%$ of training to converge to final CIR values. The proposed estimator is then used in DDCE mode for low and moderate fade channels. Simulation results show that estimation error increases with increase in fading rate.

Here, the work is advanced for fast fading channel using QR-LS joint channel estimator. Various pilot interpolation methods from previous works are compared to provide a refrence. As seen from simulation results, various interpolation techniques like MMSE, linear, spline, cubic spline, DFT-IDFT perform equally since pilots are scattered with consideration of coherence time and coherence bandwidth in time frequency grid. Based on simulation results, linear interpolation method is chosen for comparison since its complexity is the lowest among all. Performance results show that simulation results of QR-LS Coarse-Fine estimator gives better BER performance compared to pilot linear interpolation based estimation. At the same time, pilot based linear estimation needs different configurations depending on slow or fast channel conditions. Simulation results also show that proposed method outperforms QR-RLS DDCE method under fast fading environment.

In the second part, the EVS problem is mitigated effectively by providing two solutions.

In the first solution, candidate vector set of QR-LRL MIMO detector is effectively enlarged by trying every constellation point at each layer while keeping the error propagation low. Selection of least M distance candidates reduces error propagation at higher layer detection. Simulation results show that the proposed method outperforms all previous QR methods while matching soft ML and QR-DD [26] BER performance. It also achieves significant gain over original QR-LRL based soft output generation $\approx$ ($1.5dB$ for QPSK, $1dB$ for 16QAM), while avoiding multiple QR decomposition as in QR-DD. Overall, near soft ML performance is achieved with low complexity especially for low modulation order ($< 64QAM$), where the EVS effect is more severe on BER performance.

The other proposed solution is QR-LRL based IDD receiver. Here, Turbo gain is used to soothe the EVS problem. Simulation results show clearly that by efficiently using extrinsic gain of Turbo decoder, proper candidates are selected for soft output generation. This in turn reduces the error propagation. It also shows that significant BER performance improvement($\approx$ 1 dB gain) is achieved with 2-3 outer iterations of proposed method. At the same time, complex MIMO detectors are avoided and simple receiver design is achieved.

Bibliography

[1] Jeffrey G. Andrews, Arunabha Ghosh, and Rias Muhamed. *Fundamentals of WiMAX: Understanding Broadband Wireless Networking*. John Wiley and Sons., Wiley co., 2007.

[2] I. Barhumi, G. Leus, and M. Moonen. *Optimal training design for MIMO OFDM systems in mobile wireless channels*. IEEE Trans. Signal Process., vol. 51, pp. 1615-1624, Jun., 2003.

[3] C.Berrou, A.Glavieux, and P.Thitimajshima. *Near Shannon limit error-correcting Coding and Decoding,TURBO codes.* In Proceeding of ICC Conf., Vol.2, page 1064-1070, 1993.

[4] Yong Soo Cho, Jaekwon Kim, Won Young Yang, and Chung G. Kang. *MIMO-OFDM Wireless Communications with MATLAB*. John Wiley and Sons., Wiley co., 2010.

[5] W. Choi, R. Negi, and J.M Cioffi. *Combined ML and DFE decoding for V-BLAST system*. Proc. ICC, pp.1243-1248, Jun., 2000.

[6] S. Coleri, M. Ergen, A. Puri, and A. Bahai. *Channel estimation techniques based on pilot arrangement in OFDM systems*. IEEE Trans. Broadcasting, pp. 223-229, Sept. 2002, pp. 223-229, Sept., 2002.

[7] X. Dong, W.S. Lu, and A. Soong. *Linear interpolation in pilot assisted channel estimation for OFDM*. IEEE Trans. Wireless Commun., pp. 1910-1920, May, 2007.

[8] O. Edfors, M. Sandell, J.-J. van de Beek, S. K. Wilson, and P. O. B rjesson. *OFDM channel estimation by singular value decomposition*. IEEE Trans. Commun., vol. 46, pp. 931939, July, 1998.

[9] E. Eleftheriou and D. Falconer. *Tracking properties and Steady-State Performance of RLS Adaptive Filter Algorithms*. IEEE Trans. Acoust., Speech, Signal Proc., vol. ASSP-34, no. 5, pp 1097-1109, October, 1986.

[10] W.van Etten. *Maximum likelihood receiver for multiple channel transmission systems*. IEEE Trans. Commun., vol 24, no.2, pp. 276-283, Feb., 1976.

[11] G. J. Foschini and M. J. Gans. *On limits of wireless communications in a fading environment when using multiple antennas*. Wireless Press. Commun., vol. 6, no. 3, pp. 311.335, Mar., 1998.

[12] D. A. Gore, R. W. Jr. Health, and A. J. Paulraj. *Performance analysis of spatial multiplexing in correlated channel*. IEEE Transactions, Proc. ICC, Mar., 2002.

[13] S. Haykin, A. H. Sayed, J. R. Zeidler, P. Yee, and P. C. Wei. *Adaptive Tracking of Linear Time-Variant Systems by Extended RLS Algorithms*. IEEE Trans. Signal Process., vol.45, no. 5, May, 1997.

[14] Simon Haykin. *Adaptive filter theory*. Pearson, Pearson Edition, 2002.

[15] H.Kawai, K.Higuchi, N. Maeda, and M.Sawahashi. *Adaptive control of surviving symbol replica candidates in QRM-MLD for OFDM MIMO multiplexing*. IEEE J. Sel. Areas Commun., vol.24, no 6 pp.1130-1140, june, 2006.

[16] H.Kawai, K.Higuchi, N.Maeda, M.sawahashi, T.Ito, Y.Kaakura, A. Usihirokawa, and H.Seki. *Likelihood function for QRM-MLD suitable for soft-decision turbo decoding and its performance for OFCDM MIMO multiplexing in multipath fading channel*. IEICE Trans. Commun., vol.E88-B, no.1,pp.47-57,Jan., 2005.

[17] B. M. Hochwald and S.T. Brink. *Achieving near-capacity on a multiple-antenna channel*. IEEE Transactions on Communications, vol.51, pp.389-399, Mar., 2003.

[18] Peter Hoeher. *TCM on frequency-selective land-mobile fading channels*. In Proc. of the 5th Tirrenia International Workshop on Digital Communications, Tirrenia, Italy, Sep., 1991.

[19] Peter Hoeher, Stefan Kaiser, and Patrick Robertson. *Two-Dimentional Pilot Symbol Aided Channel Estimation by Wiener Filtering*. Acoustic Speech and Signal Processing, vol. 3, pp. 1845-1848,Apr., 1997.

[20] X. Hou, S. Li, C. Yin, and G. Yue. *Two-Dimensional Recursive Least Square Adaptive Channel Estimation for OFDM Systems*. IEEE, IEEE pp. 232-236, 2005.

[21] Meng-Han Hsieh and Che-Ho Wei. *Channel Estimation For OFDM Systems Based On COMB-Type Pilot Arracngement In Frequency Selective Fading Channels*. IEEE Trans., vol. 44, 1, pp. 217-225, Feb, 1998.

[22] Keun Chul Hwang, Sungwoo Park, Moon June, and Soon Young Yoon. *Iterative Joint Detection and Decoding for MIMO-OFDM Wireless Communications.* Proc. Of Signals,Systems and Computers, Pg. 17521756, ACSSC, 2006.

[23] IEEE. *IEEE P802.16m WLAN/MAN: Advanced Air interface*. IEEE Standards, IEEE 802.16m Draft D4, 2011.

[24] Tae-Ho Im. *MMSE-OSIC2: Signal Detection for Spatially Multiplexed MIMO Systems*. IEEE VTC Spring, pp. 1468-1472, May, 2008.

[25] J.Kim, D.Kim, , and S.Yun. *Mitigating error propagation in successive interference cancellation*. IEICE Trans.Commun., vol.E89-B,no.10,pp.2956-2960, Oct., 2006.

[26] Junghyun.Kim, Y.K.Park, and S.Bahng. *Efficient Soft-Output Generation Method for Spatially Multiplexed MIMO Systems," IEICE Trans. Commun.* IEICE Trans. Commun., vol.E92-B, no.11, pp. 3512-3515 Nov., 2009.

[27] E. Karami and M. Shiva. *Decision-Directed Recursive Least Squares MIMO Channels Tracking*. EURASIP J. Wireless Commun. Networking, vol. 2006, pp. 1-10, 2006.

[28] Kilhwan Kim, Yunho Jung, Seongjoo Lee, and Jaeseok Kim. *Efficient List Extension Algorithm Using Multiple Detection Orders for Soft-Output MIMO Detection*. IEICE Trans. Commun., vol.E95-B, no.3, March., 2012.

[29] Sun-Wook Kim and Kyun Hyon Tchah. *Performance Analysis of Adaptive Equalizer Design for OFDM Wireless LAN*. IEEE Transactions on Consumer Electronics, Vol. 50, No. 2, MAY, 2004.

[30] K.J.Kim, J.Yue, R.A.Iltis, and J.D.Gibson. *A QRD-M/Kalman filter based detection and channel estimation algorithm for MIMO-OFDM systems*. IEEE Tran. Wireless Commun., vol.4, no.2, pp.710-721, March, 2005.

[31] Jr. L. J. Cimini. *Analysis and simulation of a digital mobilechannel using orthogonal frequency division multiplexing*. IEEE Trans. Commun., vol. COM-3, pp. 665675, Jul., 1985.

[32] Heunchul Lee, Byeongsi Lee, and Inkyu Lee. *Iterative Detection and Decoding With an Improved V-BLAST for MIMO-OFDM Systems.* IEEE journal on selected areas in comm., Vol. 24, NO. 3,MARCH, 2006.

[33] Xiadong Li, Howard Huang, G.J. Foshini, and Reinaldo A. Valenzuela. *Effects of Iterative Detection and Decoding on the Performance of BLAST*. Proc. of Globecomm, Vol 2. Pp-1061-1066., 2000.

[34] Y. (G.) Li. *Pilot-symbol-aided channel estimation for OFDM in wireless systems*. IEEE Trans. Veh. Technol., vol. 49, pp. 12071215, July, 2000.

[35] Y. (G.) Li, L. J. Cimini, , and N. R. Sollenberger. *Robust channel estimation for ofdm systems with rapid dispersive fading channels*. IEEE Trans. Commun., vol. 46, pp. 902915, July, 1998.

[36] Ye (Geoffrey) Li. *Simplified Channel Estimation for OFDM Systems With Multiple Transmit Antennas*. IEEE Trans. Commun., vol. 1, No.1, Jan., 2002.

[37] M.H.Hayes. *Statistical Digital Signal Pprocessing and Modeling*. John Wiley and Sons Inc, Pearson Edition, 2002.

[38] Marc Moonen. *Reprot On QRD based Least Squares*. Dept. Elektrotechniek,kuleuven, ftp://ftp.esat.kuleuven.ac.be/pub/SISTA/moonen/reports/, 2002.

[39] S. Nakamori. *Square-root algorithms of RLS Wiener filter and fixed-point smoother in linear discrete stochastic systems*. Elsevier Inc., J.amc, April, 2008.

[40] Arogyaswami Paulraj, Rohit Nabar, and Dhananjay Gore. *Introduction to Space-Time Wireless Communications*. Cambridge university press, Wiley co., 2003.

[41] John Proakis and Masoud Salehi. *Digital Communications, 5th Edition*. McGraw-Hill Science/Engineering/Math, November, 2007.

[42] Matthias Ptzold. *Mobile fading Channels*. John Wiley and Sons., Wiley co., 2002.

[43] P.W.Wolniansky, G.J. Foschini, G.D. Golden, and R.A. Valenzuela. *V-BLAST: An architecture for realizing very high data rates over the rich-scattering wireless channel*. Proc. URSI ISSSE, pp. 295-300, Sept., 1998.

[44] G. G. Raleigh and J. M. Cioffi. *Spatio-temporal coding for wireless communication*. IEEE Trans. Commun., vol. 46, pp.357366, Mar., 1998.

[45] TheoDore S. Rappaport. *Wireless Communications: Principles and Practice*. Pearson Education Inc, Wiley co., 2002.

[46] Divyang Rawal, Seungjae Bahng, Youn-Ok-Park, C.Vijaykumar, and Hyeong-Sook Park. *Mitigating Empty Vector Set problem using Enlarged QRLRL-M based Soft SM-MIMO Detector*. Submitted To Journal, Submitted, 2013.

[47] Divyang Rawal and C.Vijaykumar. *QR-RLS Based Adaptive Channel TEQ for OFDM Wireless LAN*. IEEE Conf., ICSCN, INDIA, 2008.

[48] Divyang Rawal, Park Youn Ok, and C. vijaykumar. *A Novel Training based QR-RLS channel estimator for OFDM-MIMO systems*. IEEE conf. Page 1-4., WiAd U.K., 2010.

[49] Divyang Rawal, Youn-Ok Park, C.Vijaykumar, Hyeong Sook Park, and Hoon Lee. *A Joint QR-LS based Coarse-Fine channel estimation and QR-LRL detection For Mobile Wimax 802.16m*. IEEE COMSOC, GlobeCom , Pg. 1-5, Dec. 5-9, 2011.

[50] Divyang Rawal, Youn-Ok-Park, Seungjae Bahng, Hoon Lee, Choi-Jung Pil, and C.Vijaykumar. *Efficiently using extrinsic gain for candidate vectors selection in QR-LRL based IDD MIMO receiver*. IEEE Conf., ICTC, S.Korea, 2012.

[51] T. Roman, M. Enescu, and V. Koivunen. *Time-Domain Method for Tracking Dispersive Channels in MIMO OFDM Systems*. in Proc. IEEE Conf. Acoustics, Speech, and Signal Process., vol. 4,pp. 393.396, 2003.

[52] M. A. Saeed, N. K. Noordin, S. Khatun B. M. Ali, and M. Ismail. *RLS Channel Estimation and Tracking for MIMOextended IEEE 802.11a WLANs*. IJCSNS International Journal of Computer Science and Network Security, VOL.8 No.2, February, 2008.

[53] S. Sanhdu and A. Paulraj. *Space-time block codes: a capacity perspective*. IEEE Commun. Letter, vol.4 no.12, pp.384-386, Dec., 2000.

[54] S.BAHNG, Y.K.Park, and J.Kim. *QR-LRL Detection for Spatially Multiplexed MIMO Systems*. IEICE Trans. Commun., vol.E91-B, no.lO, 2008.

[55] D. Schafhuber, G. Matz, and F. Hlawatsch. *Adaptive Wiener filters for time-varying channel estimation in wireless OFDM systems*. IEEE Proc. Conf., vol. 4, pp. 688-691, 2003.

[56] Bernard Sklar. *Digital Communications: Fundamentals and Applications*. Pearson Education Inc, Wiley co., 2001.

[57] Gordon L. Stuber. *Principles of Digital Communication*. Springer, Kluwer Academic Publishers, 2001.

[58] A. L. Swindlehurst and G. Leus. *Blind and semi-blind equalization for generalized spacetime block codes*. IEEE Trans. Signal Process., vol. 50, no. 10, pp. 24892498, Oct., 2002.

[59] V. Tarokh. *Space.time block codes from orthogonal designs*. IEEE Trans.Inform. Theory, vol. 45, pp. 1456.1467, July, 1999.

[60] I. E. Telatar. *Capacity of multi-antenna Gaussian channels*. Eur. Trans.Telecommun., vol. 10, pp. 585.595, Nov., 1999.

[61] Truong TK, Wang LJ, Reed IS, and Hsieh WS. *Image data compression using cubic convolution spline interpolation*. IEEE Trans. on Image Process., 1988-95, Nov., 2000.

[62] F. Tufvesson and T. Maseng. *Pilot assisted channel estimation for OFDM in mobile cellular systems*. Proc. IEEE VTC97, pp. 1639-1643, May, 1997.

[63] J.-J. van de Beek, O. Edfors, M. Sandell, S. K. Wilson, and P. O.Borjesson. *On channel estimation In OFDM systems*. VTC 96, pp.815-819, Nov., 1996.

[64] W.C.Jakes. *Microwave Mobile Communications*. Wiley, New York, 1974.

[65] W.Shin, H.Kim, Mi hyun Son, and H.Park. *An Improved LLR Computation for QRM-MLD in Coded MIMO systems*. Proc. VTC, pp.447-451 Fall, 2007.

[66] Fuqin Xiong. *Digital Modulation Techniques (Communications/Networking)*. Artech House, 2nd Revised edition edition (May 2006), Wiley co., 2006.

[67] Y. Zhao and A. Huang. *A novel channel estimation method for OFDM mobile communication systems based on pilot signals and transform-domain processing*. Proc. IEEE VTC97, pp. 1639-1643, May, 1997.

[68] S. Zhou, B. Muquet, and G. B. Giannakis. *Subspace-based (semi-) blind channel estimation for block precoded spacetime OFDM*. IEEE Trans. Signal Process., , vol. 50, no. 5, pp. 12151228, May, 2002.

[69] Ernesto Zimmerman and Gerhard Fettweis. *Adaptive Vs Hybrid Iterative MIMO Receivers Based On MMSE Linear And Soft-SIC Detection*. Proceedings of PIMRC, pg. 1-5, 2006.

Appendix 1

.1 Error Minimization Mehods and Adaptive Equalixer Updating

Suppose $d(n)$ is transmitted through wireless channel $h(n)$ given by Eq. (2.1), then the received signal for ($CIR > CP$)is given by

$$X(n) = (d(n) * h(n)) + v(n) + i(n)$$

where $i(n)$ is the ISI and $v(n)$ is additive white gaussian noise.
To get back the desired signal $d(n)$, a TEQ (inverse filter) with filter taps w(n) is employed at the front end of the receiver. This not only nullifies the channel's response but also divides noise and ISI produced by the channel. The signal at the output of TEQ is given by

$$\hat{d}(n) = X(n) * w(n),$$

The difference between the desired signal $d(n)$ and the obtained signal $\hat{d}(n)$ at the output of TEQ is the error signal $e(n)$ and is given by

$$e(n) = d(n) - \hat{d}(n) = d(n) - (w(n) * X(n))$$

where d(n) is instantaneous value of desired signal ,
$w(n) = [w_n(0)w_n(1)w_n(2)...w_n(p)]$
$X^T(n) = [x_n(0)x_n(1)x_2(n)...x_n(p)]$ at time n.
where p shows the order of the FIR filter. Generally it range between $(CIR-CP, CIR)$ to provide optimum inverse filter. The error e(n) is minimized using MMSE, LSE based method and used to update coefficients of TEQ, such that it better approximates $\hat{d}(n)$ to $d(n)$ from obtained signal $X(n)$.

.1.1 MMSE Error Based Adaptive Updating

The mean square error [14][37] given by

$$\zeta(n) = E|e(n)|^2 \tag{1}$$

$\zeta(n)$ is minimized by differentiating it with respect to equalizer coefficients $w(n)$ at time n and equating it to zero. The resultant equation is

$$E[d(n) - \sum_{l=0}^{p} w_n(l)x(n-l)]x^*(n-k) = 0 \tag{2}$$

$$R_x(n)w(n) = r_{dx}(n)$$

The solution of the above equation gives the optimum value for the tap coefficients $w(n)$. Here $R_x(n)$ is the autocorrelation matrix of dimension $(p+1) \times (p+1)$ of the obtained signal and $r_{dx}(n)$ is the cross correlation matrix of $p+1$ between desired signal and the obtained signal at time n, where p is channel length L as in Eq. (2.1)

.1.2 Least Mean Square(LMS) Based Updating

Since all the statistical information required to find out the solution of Eq. (2) is not available, LMS replaces it by instantaneous value of the signal. The optimum coefficients are updated by the recursive equation

$$w(n+1) = w(n) + \mu e(n)X^*(n)$$

where μ is the convergence parameter and it's value is dependent on the eigen spread of the obtained data vector $x(n)$. Generally μ is kept between $0 < \mu < \frac{2}{traceR_x(n)}$ for stable and faster convergence.

.1.3 Standard RLS Based Updating

In LMS the expectation is replaced by instantaneous value. Due to this, convergence is slow and MSE is not sufficiently minimum. To overcome this and increase the convergence, the expectation term of Eq. (1) is replaced by summation and a forgetting factor λ with value varying from $(0 \rightarrow 1)$. The resultant weighted least square error at time n is given by

$$\zeta(n) = \sum_{i=0}^{n} \lambda^{n-i}|e(i)|^2, \tag{3}$$

where $e(i) = d(i) - (w(i) * x(i))$. The difference between this and previous (LMS) method is that the optimum filter coefficients found by minimizing Eq. (3) are purely data dependent, i.e. even if the obtained data vector at different times has same statistical properties, the optimum tap coefficients may differ due to variation in data. By differentiating Eq. (3) w.r.t to tap coefficients

w(n) and equating it with zero provides the optimum solution given by

$$w(n) = R_x^{-1}(n) r_{dx}(n) \tag{4}$$

where R_x is auto correlation matrix of channel output vector,
$X^T(n) = [x(0, x(1)...x(n)]$ and r_{dx} is cross correlation vector between desired $D = [d(0), d(1)...d(n)]$ and channel output/received data vector at time n. Instead of finding inverse of R_x woolbury's identity is used, as given by

$$(A + UV^H)^{-1} = A^{-1} - \frac{A^{-1}UV^H A^{-1}}{1 + V^H A^{-1} U}$$

where $U = V^T = X = [x(0), x(1).....x(n)]$ is prewindowing data of obtained vector. A recursive solution [37][14] for tap coefficient update is given by,

$$w_n = w_{n-1} + G(n)[d(n) - w_{n-1}^T x(n)] \tag{5}$$

where $P(n) = R_x(n)^{-1}$,

$$P(n) = \lambda^{-1}[P(n-1) - G(n)x^T(n)P(n-1)]$$

and G(n) is gain vector given by

$$G(n) = \frac{\lambda^{-1}P(n-1)x^*(n)}{1 + \lambda^{-1}x^T(n)P(n-1)x^*(n)}$$

The term $R_x = (X^T X)$ in Eq. (4) is extremely damaging from a numerical point of view because the squaring doubles the dynamic range or word-length or accuracy becomes half. To avoid this, R_x is decomposed with the help of QR [14] decomposition which results in QR based equalizer. This avoids matrix inversion as well as roundoff errors.

Appendix 2

.2 Various Hard ML OSIC Detection Methods

The ordering criterion is very important in OSIC based detection and it depends on the cancellation method. For example, post detection SNR is the optimal criterion in ZF-OSIC and post detection SINR is the optimal criterion in MMSE-OSIC.

MMSE-OSIC Method

The goal of MMSE-OSIC detection method is to increase the performance by combining the MMSE filter and OSIC method. The MMSE filter, minimizing the interference is described below:

$$\mathbf{G}^{(1)} = (((\mathbf{H}(1))^H \mathbf{H}^{(1)} + {\sigma_z}^2 I)^{-1} (\mathbf{H}^{(1)})^H, \mathbf{H}(1) = [h_1, h_2, , h_m] \tag{6}$$

where, ${g_k}^{(i)}$ is the k^{th} row of $\mathbf{G}^{(i)}$; ${h_k}^{(i)}$ is the k^{th} column of $\mathbf{H}^{(i)}$, and ${SINR^{(i)}}_j$ is j^{th} SINR value of i^{th} $\mathbf{G}^{(i)}$ and $\mathbf{H}^{(i)}$. From Table (1), it is observed that the MMSE filter and the post detection $SINR$ ordering are used to mitigate the error propagation and interference. However, the MMSE-OSIC still suffers from significant performance degradation due to inaccurate detection of the first layer symbol.

QR-OSIC Method

It is well known that the cancellation ordering dominates the overall performance in OSIC detection method. Since ZF-OSIC is used for interference cancellation in conventional OSIC, post detection SNR is used for ordering criterion. The post detection SNR value is given as follows:

$$\zeta_i = \parallel \mathbf{G}(i,:) \parallel^2, {}_{i=1,2,\ldots,m,} \mathbf{G} = (\mathbf{H}^H \mathbf{H})^{-1} \mathbf{H}^H \tag{7}$$

where, ζ_i denotes the post detection SNR value of i^{th} layer. The example of conventional OSIC ordering process for 4×4 MIMO system is described in Fig. (1). After ordering, the system equation is given by

$$\mathbf{y} = \mathbf{H}_{ordered} \cdot \mathbf{x}_{ordered} + \mathbf{z} \tag{8}$$

Table 1: Psuedo code for MMSE-OSIC SM-MIMO Detector .

$function[\hat{x}] = MMSE - OSIC(\mathbf{y}, \mathbf{H}^{(1)}, \mathbf{G}^{(1)})$
$k = argmax_j \mathbf{SINR}^{(1)}{}_j$
$fori = 1 : m$
$x_k = g^{(i)}{}_k y^{(i)}$
$\hat{x}_k = Q(x_k)$
$\mathbf{y}^{(i+1)} = \mathbf{y}^{(i)} - h^{(i)}{}_k \hat{x}_k$
$\mathbf{H}^{(i+1)} = [h^{(i)}{}_1, h^{(i)}{}_2, , h^{(i)}{}_{k-1}, h^{(i)}{}_{k+1}, , h^{(i)}{}_{m-i+1}]$
$\mathbf{G}(i+1) = (((\mathbf{H}(i+1))^H \mathbf{H}(i+1) + \sigma^2{}_z I)^{-1} (\mathbf{H}(i+1))^H$
$k = argmax_j SINR^{(i+1)}{}_j$
$\hat{x}(i) = \hat{x}_k$
end

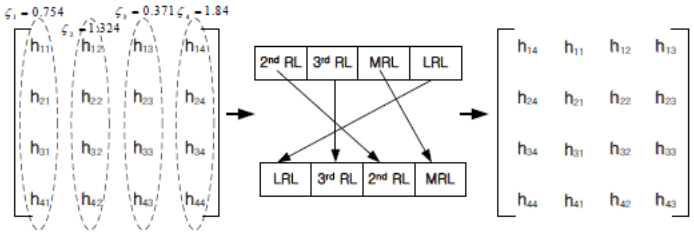

Figure 1: Example of Conventional ordering method 4×4 MIMO method

$$\mathbf{H}_{ordered} = [h_{(1)}^{LRL} ... h_{(m-1)}^{2ndRL} h_{(m)}^{MRL}] \tag{9}$$

$$\mathbf{x}_{ordered} = [x_{(1)}^{LRL} ... x_{(m-1)}^{2ndRL} x_{(m)}^{MRL}] \tag{10}$$

where, subscript (i) denotes the i^{th} column vector or i^{th} symbol after ordering, respectively. Superscript i^{th} RL denotes the layer or symbol corresponding to i^{th} reliable layer and symbol before ordering, respectively. If a 4×4 MIMO system is assumed, then cancellation method involving QR decomposition is given as follows:

$$\mathbf{H}_{ordered} = Q \cdot R \tag{11}$$

where, Q is a 4×4 unitary matrix, and R is a 4×4 upper triangular matrix. Multiplying both sides with Q^H, the system equation is given by

Table 2: Psuedo code for QR-OSIC .

$\hat{x}_{(4)} = Q(\frac{y_4}{r_{44}})$
$\hat{x}_{(3)} = Q(\frac{\bar{y}_3 - r_{34}x_{(4)}}{r_{33}})$
$\hat{x}_{(2)} = Q(\frac{\bar{y}_2 - r_{23}x_{(3)} - r_{24}x_{(4)}}{r_{22}})$
$\hat{x}_{(1)} = Q(\frac{\bar{y}_1 - r_{12}x_{(2)} - r_{13}x_{(3)} - r_{14}x_{(4)}}{r_{11}})$
$\mathbf{x}_{ordered} = \left[\hat{x}_1 \hat{x}_2 \hat{x}_3 \hat{x}_4\right]^T$

$$\bar{\mathbf{y}} = Q^H(\mathbf{H}_{ordered}\mathbf{x}_{ordered} + z) = R\mathbf{x}_{ordered} + \bar{\mathbf{z}} \tag{12}$$

$$\begin{pmatrix} y_1 \\ y_2 \\ y_3 \\ y_4 \end{pmatrix} = \begin{pmatrix} h_{1,1} & h_{1,2} & h_{1,3} & h_{1,4} \\ h_{2,1} & h_{2,2} & h_{2,3} & h_{2,4} \\ h_{3,1} & h_{3,2} & h_{3,3} & h_{3,4} \\ h_{4,1} & h_{4,2} & h_{4,3} & h_{4,4} \end{pmatrix} \begin{pmatrix} x_1 \\ x_2 \\ x_3 \\ x_4 \end{pmatrix}$$

where, $\bar{\mathbf{y}} = Q^H\mathbf{y}$, $\hat{\mathbf{z}} = Q^H\mathbf{z}$.

The pseudo code for the OSIC is given in Table (2). From Table (2), it is observed that the first detected symbol is assumed to be correct and is used to eliminate the co-channel interference. Therefore, it is important to exactly detect the first layer symbol. Otherwise, error propagation will occur. That is why the most reliable layer (MRL) is chosen as the first layer for detection in ordering of OSIC.

.2.1 QR-MRL Algorithm

As mentioned in the above section, proper ordering improves the overall performance of OSIC. Pseudo code for QR-MRL detection method is summarized in Table (3). From Table (3), it can be seen that instead of deciding the first symbol as in conventional QR-OSIC method, all constellation points are tried as the first layer symbol. Thus QR-MRL can exactly detect the first layer symbol and the error propagation is significantly reduced compared to conventional OSIC method. After all the symbols are tried, the minimum distance vector is chosen as optimum to achieve hard ML performance.

Table 3: Psuedo code for QR-MRL .

$fori = 1 :\parallel C \parallel$
$\hat{x}_{(4)} = C(i)$
$\hat{x}_{(3)} = Q(\frac{\bar{y}_3 - r_{34}x_{(4)}}{r_{33}})$
$\hat{x}_{(2)} = Q(\frac{\bar{y}_2 - r_{23}x_{(3)} - r_{24}x_{(4)}}{r_{22}})$
$\hat{x}_{(1)} = Q(\frac{\bar{y}_1 - r_{12}x_{(2)} - r_{13}x_{(3)} - r_{14}x_{(4)}}{r_{11}})$
$\mathbf{x}_{ordered} = [\hat{x}_1\hat{x}_2\hat{x}_3\hat{x}_4]^T$
$ifMetric < BigNumber$
$BigNumber = Metric$
$\hat{\mathbf{x}}_{ordered} = Metric$
end
end

.2.2 QRM-MLD Detection Algorithm

In QRM-MLD detection method, all constellation points are considered as all layer symbols via breadth-first search algorithm. Although QRM-MLD can exactly detect the first layer symbol compared to conventional OSIC, a large number of candidate vectors are required in order to achieve hard-output ML performance. If a 4×4 MIMO system is assumed, the detailed description of QRM-MLD is described as follows:

After the ordering process based on the $\parallel h_k \parallel^2$, $(k = 1, 2, 3, 4)$, 4×4 ordered (as in Fig. (1), except instead of SINR, ordering is based on SNR so it is in reverse order of Fig.1), channel matrix $\mathbf{H}_{ordered}$ is decomposed as where, $\bar{\mathbf{y}} = Q^{\mathbf{H}}\mathbf{y}$, $\bar{\mathbf{z}} = Q^{\mathbf{H}}\mathbf{z}$. After obtaining system equation Eq.(12), all the constellation points are assigned to the first layer symbol. Then, select the transmitted candidate vector set $[x_{4,(1)}, ..., x_{4,(M)}]$ from the all possible candidate vector sets $[x_{4,(1)}, x_{4,(2)}, ..., x_{4,(|C|)}]$, where $|C|$ is the number of elements of the constellation point set. The ML metric is then used for candidate vector selection which will be transferred to the next layer. The ML metric is calculated as follows:

$$|\bar{y}_4 - r_{44}x_{4,(k)}|2, k = 1, 2, ..., |C| \tag{13}$$

After selecting the M candidate vectors that correspond to the least M value of metric, the each selected candidate vector is expanded into the second layer and $M|C|$ ML metric calculation is performed using Eq. (13).

$$\begin{pmatrix} y_1 \\ y_2 \end{pmatrix} - \begin{pmatrix} r_{3,3} & r_{3,4} \\ 0 & r_{3,4} \end{pmatrix} \begin{pmatrix} x_{3,(k)} \\ x_{4,(k)} \end{pmatrix}$$

Again, M candidate vectors corresponding to the smallest M metric values out of $M|C|$ vector set are chosen for the transmitted signal $[x_3\ x_4]^T$. This process will continue till the last layer. After obtaining the final candidate vectors for transmitted signal $[x_1\ x_2\ x_3\ x_4]^T$ at the last layer, the transmitted signal corresponding to the minimum metric value is determined. The performance of QRM-MLD method depends on the M parameter which decides the number of candidate vectors. A large M parameter value can achieve the hard-output ML performance. However it increases the complexity tremendously.